國 立 交 通 大 學

電信工程學系碩士班
碩士論文

IEEE 802.16 OFDMA 基頻傳收機設計與實現

Design and Implementation of IEEE 802.16
OFDMA Baseband Transceiver

研 究 生：龍星宇　　　　　　　Student：Hsing-Yu Lung

指導教授：吳文榕 博士　　　　Advisor：Dr. Wen-Rong Wu

中華民國九十五年七月

IEEE 802.16 OFDMA 基頻傳收機設計與實現

Design and Implementation of IEEE 802.16

OFDMA Baseband Transceiver

研 究 生：龍星宇　　　　　　Student：Hsing-Yu Lung

指導教授：吳文榕 博士　　　　Advisor：Dr. Wen-Rong Wu

國 立 交 通 大 學

電信工程學系碩士班

碩 士 論 文

A Thesis

Submitted to Department of Communication Engineering

College of Electrical Engineering and Computer Science

National Chiao-Tung University

in Partial Fulfillment of the Requirements

for the Degree of

Master of Science

In

Communication Engineering

July 2006

Hsinchu, Taiwan, Republic of China

中華民國九十五年七月

IEEE 802.16 OFDMA 基頻傳收機之設計與實現

Design and Implementation of IEEE 802.16

OFDMA Baseband Transceiver

研究生：龍星宇　　　　　　　　　指導教授：吳文榕 教授

國立交通大學電信工程學系碩士班

中文摘要

　　IEEE 802.16 標準被視為下一代的無線通訊系統。在此篇論文之中，我們著重於其中之一種基頻傳收機的設計與實做：正交分頻多工存取(OFDMA)，傳送端有通道編碼、調變與子載波配置等功能，在接收端結合了前端接收機以及後端接收機來解調信號，前端接收機實做出同步與通道估計而後端接收機則實做出等化器、解碼與復原子載波配置等功能，並納入一些通道效應以模擬真實的通訊環境。整個以 MATLAB 環境建立的模擬平台可以順利地執行，模擬結果顯示其接收機可在高達每小時一百公里的行動環境下運作。

Design and Implementation of IEEE 802.16

OFDMA Baseband Transceiver

Student: Hsing-Yu Lung   Advisor: Dr. Wen-Rong Wu

Department of Communication Engineering

National Chiao-Tung University

Abstract

IEEE 802.16 has been considered as a standard for the next generation wireless communication system. In this thesis, we focus on the design and implementation of a baseband transceiver for a multiple access mode in 802.16, the orthogonal division multiplexing access (OFDMA). The main functions conducted by the transmitter include channel coding/modulation and subcarrier allocation. In the receiver side, an inner and an outer receiver are designed to jointly demodulate the received signal. The inner receiver performs synchronization and channel estimation, while the outer receiver performs equalization, decoding, and subcarrier de-allocation. We consider the downlink scenario and use SCM as our channel mode. A platform with the MATLAB environment is built such that system simulations can be easily conducted. Simulations show that the designed OFDMA receiver can be operated with a mobile speed up to 100Km/hr.

Acknowledgment

I would like to acknowledge the guidance and patience of my advisor, Dr.

Wen-Rong Wu. I also thank my friends for their encouragement and help.

Catalog

Figure List

Table List

Abbreviations and Acronyms

3GPP	3rd Generation Partnership Project
AAS	adaptive antenna system
ADC	analog to digital converter
AMC	advanced modulated coding
BS	base station
CFO	carrier frequency offset
CP	cyclic prefix
DAC	digital to analog converter
DC	direct current
DFT	discrete Fourier transform
DL-MAP	downlink map
FCH	frame control header
FDD	frequency division duplex
FEC	forward error correction
FFT	fast Fourier transform
FUSC	fully usage of subchannels
IDcell	identification of cells
IDFT	inverse discrete Fourier transform
IFFT	inverse fast Fourier transform
LSB	least significant bit
MAC	medium access control layer
MSB	most significant bit
NLOS	non-light-of-sight
OFDM	orthogonal frequency division multiplexing

OFDMA	orthogonal frequency division multiplex access
PHY	physical layer
PN	pseudo-noise
PRBS	pseudo-random binary sequence
PUSC	partial usage of subchannels
RF	radio frequency
SC	single carrier
SCM	spatial channel model
SDMA	space division multiplex access
SFO	sampling frequency offset
SNR	signal-to-noise ratio
SS	subscriber station
STC	space time coding
TDD	time division duplex
TUSC	tile usage of subchannels
UL-MAP	uplink map
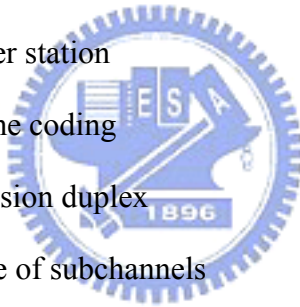
Chapter 1: Introduction

When telegram and telephone were invented, messages could be transmitted through electric wires. Although these technologies are amazing, transmission wires limited transmission areas and mobility. Into the wireless era, communication is can be taken place in any place and any time. Originally, communication is mainly used for voice transmission. As the computer age comes, it is gradually evolved for data transmission. Wireless communication is considered as one of the most important technologies human being ever invented. Many standards have been developed for different technologies and different purposes. Figure 1-1 shows the distribution of current standards for wireless communications.
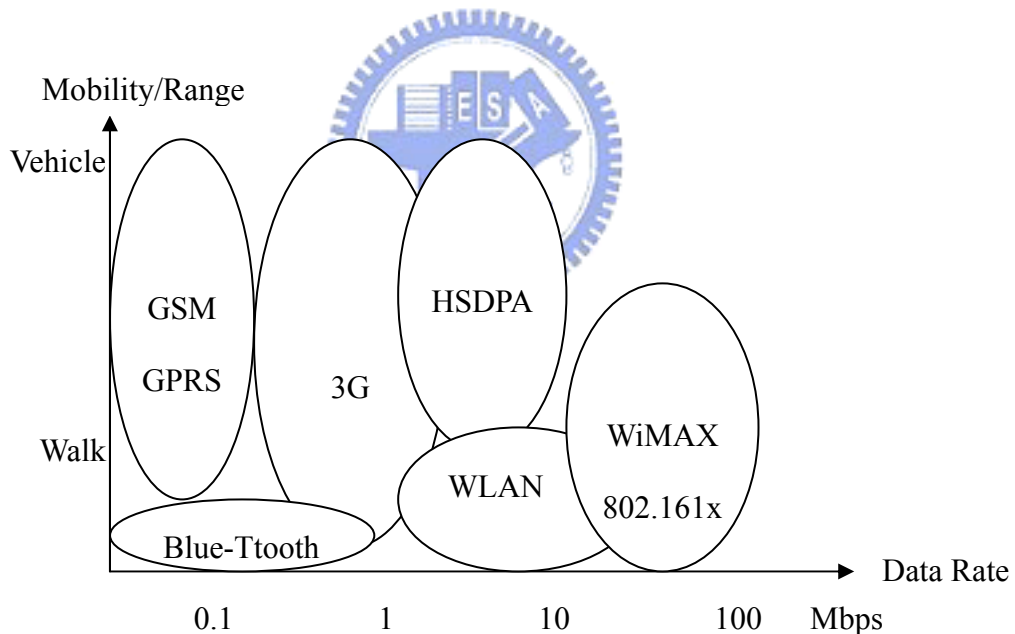
Figure 1-1 : The wireless communication standards

This thesis focuses on the development of the baseband transceiver for wireless metropolitan area network (WMAN). Right now, the IEEE 802.16 is considered to be the most popular standard for WMAN. The WiMax forum, supported by many international corporations, is a well-known organization studying the application

aspects of IEEE 802.16. IEEE 802.16 was first approved in December 2001 and followed by three amendments: 802.16a, 802.16b, and 802.16c. In September 2003, a 802.16REVd project aimed to combine the earlier 802.16 documents including the a/b/c amendments was initiated. This project concluded in 2004 with the release of 802.16-2004 [2] . In order to cover the mobility applications, the amendment 802.16e [3] was proposed and rectified recently. Since its large coverage and higher data rate, 802.16e can be further considered to be one of the next generation wireless communication systems.

Orthogonal frequency division multiplexing (OFDM) has been considered as an efficient communication technique evolved from frequency-division multiplexing (FDM) [5] ; it can be seen as one kind of multi-carrier system. The orthogonal property of between subcarriers gives the optimal bandwidth efficiency. In 1971, FFT and guard interval was introduced into OFDM [6] , efficient realization of OFDM systems become feasible. Moreover, the concept of cyclic prefix [7] effectively solves the inter symbol interference (ISI) and the fading channel problem. Today, OFDM is widely used in many communication systems such as ADSL, DVB, UWB, and WLAN. Orthogonal frequency division multiple access (OFDMA) is a multiple access scheme that bases on OFDM systems. Multiple access is achieved with a 2-dimension partitioning of subcarriers and symbols (frequency and time).

This research concentrates on the baseband transceiver design for the OFDMA mode in IEEE 802.16 specification. We first build the transmitter and the receiver, including the channel model, the inner receiver, and the outer receiver. Then, we analyze the impact of channel effects and show that typical solutions [8] [12] [12] [13] [13] for inner receiver design may not be able to meet the performance requirement. Thus, we proposed new algorithms to improve the performance. Finally, system

simulations are conducted to show the effectiveness of the proposed algorithms.

The organization of the rest of the thesis is shown as follows. In Chapter 2, the PHY layer of 802.16 is described in detail. In Chapter 3, the inner receiver and synchronization algorithms are developed. In Chapter 4, simulation results are shown. Then, we draw conclusions in Chapter 5.

Chapter 2: OFDMA PHY Mode

The reference model of IEEE 802.16 comprises 2 levels: medium access control (MAC) layer and physical (PHY) layer. The PHY layer refers to network hardware, electromagnetic connection, and other low-level functions. The PHY of 802.16e includes multiple specifications such as, single carrier (SC), SCa, OFDM, and OFDMA, each appropriate to a particular frequency range and application. Here, we chose OFDMA for our study since it is used in the mobile mode, 802.16e. OFDMA is designed for multiple access in non-line-of-sight (NLOS) operation in the frequency bands below 11 GHz. For licensed bands, channel bandwidth should be limited to the regulatory provisioned bandwidth divided by any power of 2 no less than 1.0 MHz.

2.1 System Structure

2.1.1 Symbol Description

(A) Time domain symbol

Inverse-Fourier-transforming of a frequency domain symbol creates the OFDMA time domain symbol. This time duration is referred to as the useful symbol time T_b. A copy of the last T_g of the useful symbol period, termed CP, is added in front of the original symbol; it is used to resist channel effect, while maintaining the orthogonality of the subcarriers. Figure 2-1 illustrates this structure.
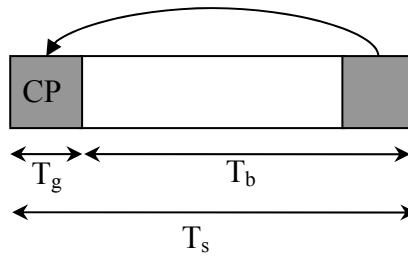
Figure 2-1 : OFDMA symbol time structure

(B) Frequency domain symbol

An OFDMA symbol is made up of subcarriers, the number of which determines the FFT size; sizes of 2048, 1024, 512, and 128 are supported. However, the thesis considers the FFT size of 2048 only. There are several subcarrier types:

- Data subcarriers: for data transmission
- Pilot subcarriers: for various synchronization/estimation purposes
- Null subcarriers: no transmission, for guard bands and DC carrier

The purpose of the guard bands is to enable the signal to naturally decay and create the FFT "brick wall" shaping. In the OFDMA mode, the active subcarriers are divided into the subsets of the subcarriers; each subset is termed a subchannel. In the downlink, a subchannel may be intended for different receivers; in the uplink, a transmitter may be assigned to one or more subchannels. The subcarriers forming one subchannel may not be adjacent. The concept of subchannelization is shown in Figure 2-2.
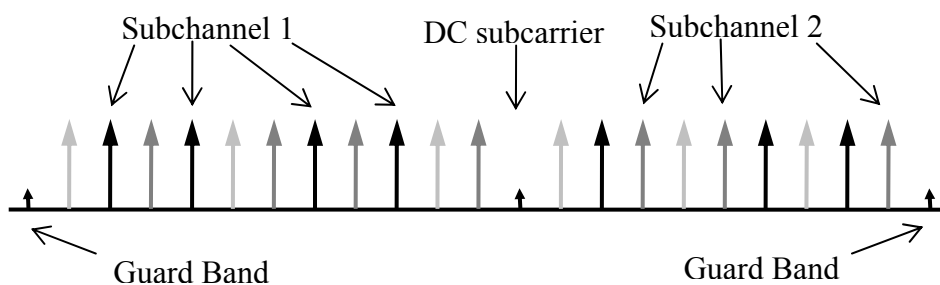
Figure 2-2 : OFDMA frequency description

2.1.2 Frame Structure

In licensed bands, the duplexing method should be either frequency division duplex (FDD) or time division duplex (TDD). In license-exempt bands, the duplexing method should be TDD. An OFDMA PHY burst, either a downlink burst or an uplink burst, carries MAC messages, i.e. MAC PDUs. Figure 2-3 shows the frame structure with TDD.
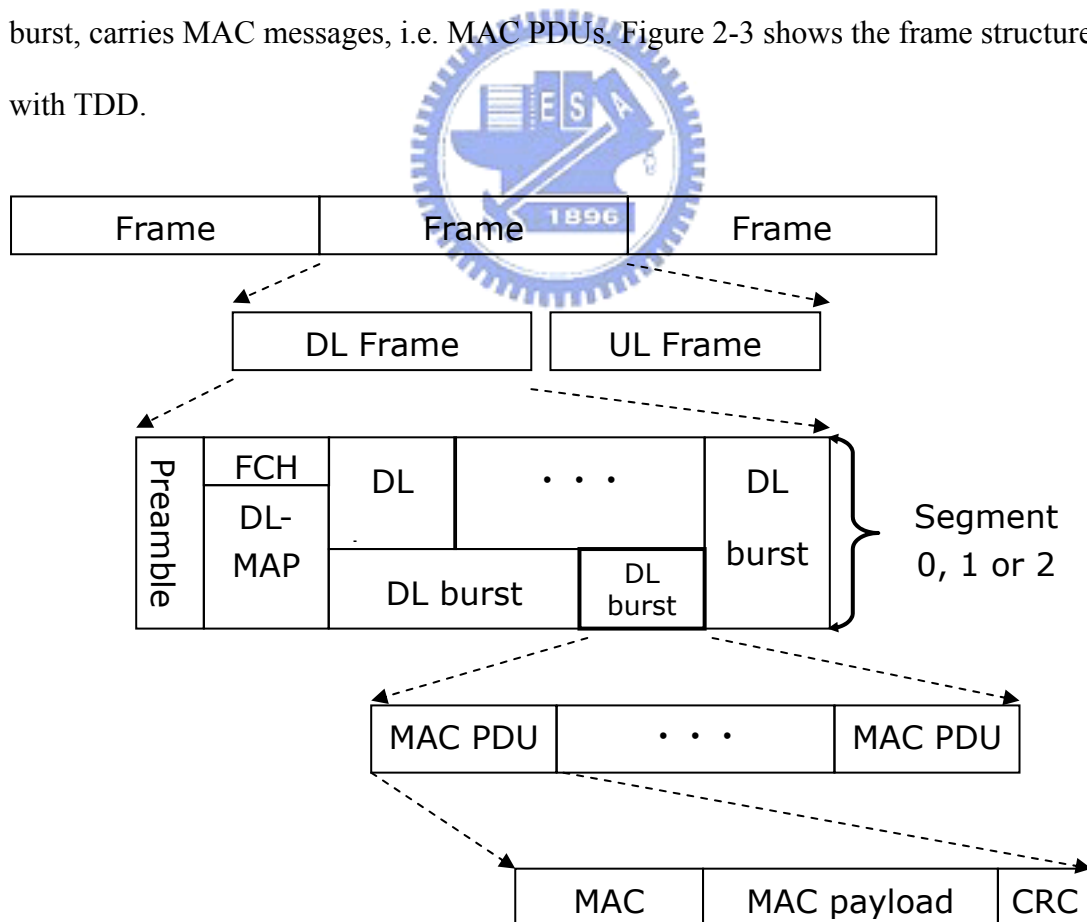
Figure 2-3 : OFDMA Frame data structure

When implementing a TDD system, the frame structure is built both for base station (BS) and subscriber station (SS) transmissions. Each frame in the downlink transmission begins with a preamble followed by a DL (downlink) period and an UL (uplink) period. In each frame, the transmit transition gap (TTG) and the receive transition gap (RTG), as

Figure 2-4, should be inserted between the downlink and uplink and at the end of each frame, respectively, to allow the BS to turn around.
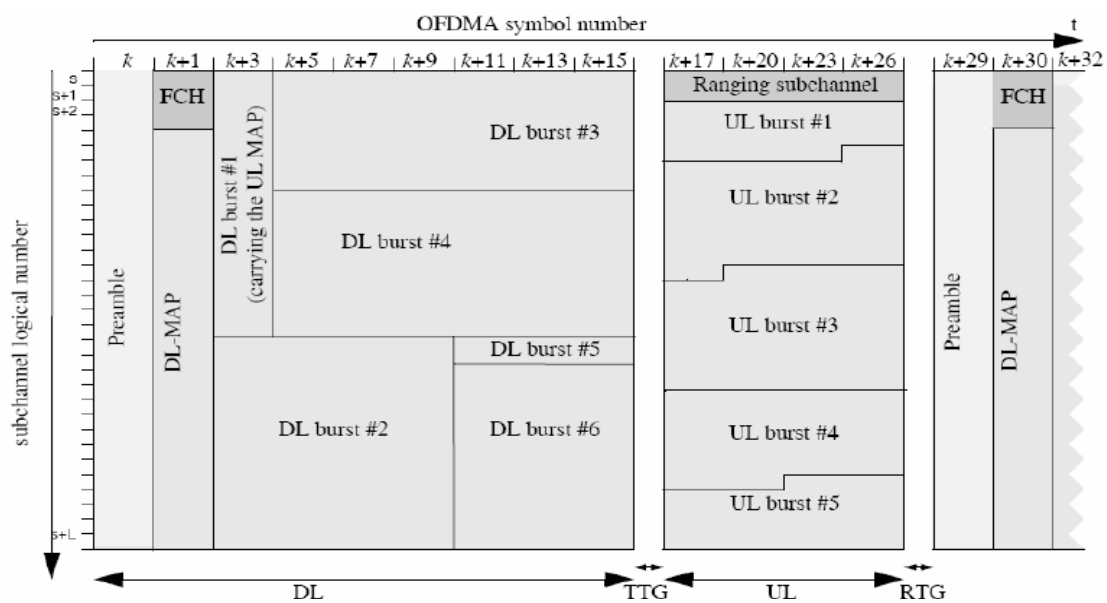
Figure 2-4 : Time plan (one TDD time frame)

2.1.3 Unit

There are various processing units in OFDMA mode. Since the data are mapped on both time and frequency domains in OFDMA systems, some units are two-dimensional and others are the one-dimension either on the frequency domain or the time domain.

The "subcarrier" is the most basic unit and composes all other units. The "OFDMA symbol" is the one-dimension unit and comprises one symbol on time domain. The "subchannel" is the one-dimension unit and comprises certain

subcarriers in frequency domain. Generally, the "subcarrier" is used for the basic frequency unit and the "OFDMA symbol" is used for the basic time unit. The two-dimension (2D) units range from large to small are the "frame", "sub-frame", "zone", "segment", "burst", "slot", and "cluster". The definitions of these units, depending on the OFDMA symbol structure, are different for uplink and downlink, and also different for different subcarrier allocation methods. The detail of these units will be explained in later sections. Figure 2-5 depicts the relationship of these units.

A **frame** is a structure data sequence and contains both the uplink sub-frame and the downlink sub-frame.

A **sub-frame** is a smaller frame in a frame for uplink or downlink.

A **zone** is a region of contiguous OFDMA symbols for which the same subcarrier allocation scheme is applied. A sub-frame may have multiple subcarrier allocation schemes.
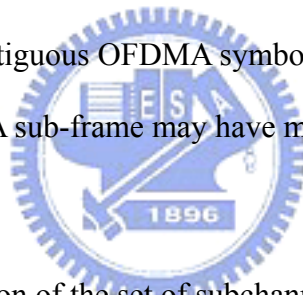
A **Segment** is a subdivision of the set of subchannels for certain particular allocation zone. One segment is used for deploying a single instance of the MAC.

A **burst** is a region of contiguous subchannels and OFDMA symbols and contains broadcast data or unicast data for corresponding users.

A **slot** a two-dimensional unit and is the minimum possible "data" allocation unit. The amount of corresponding frequency subcarriers is equal to a "subchannel".

A **cluster** is a half of a slot (divided in frequency) for a procedure in one particular subcarrier allocation.
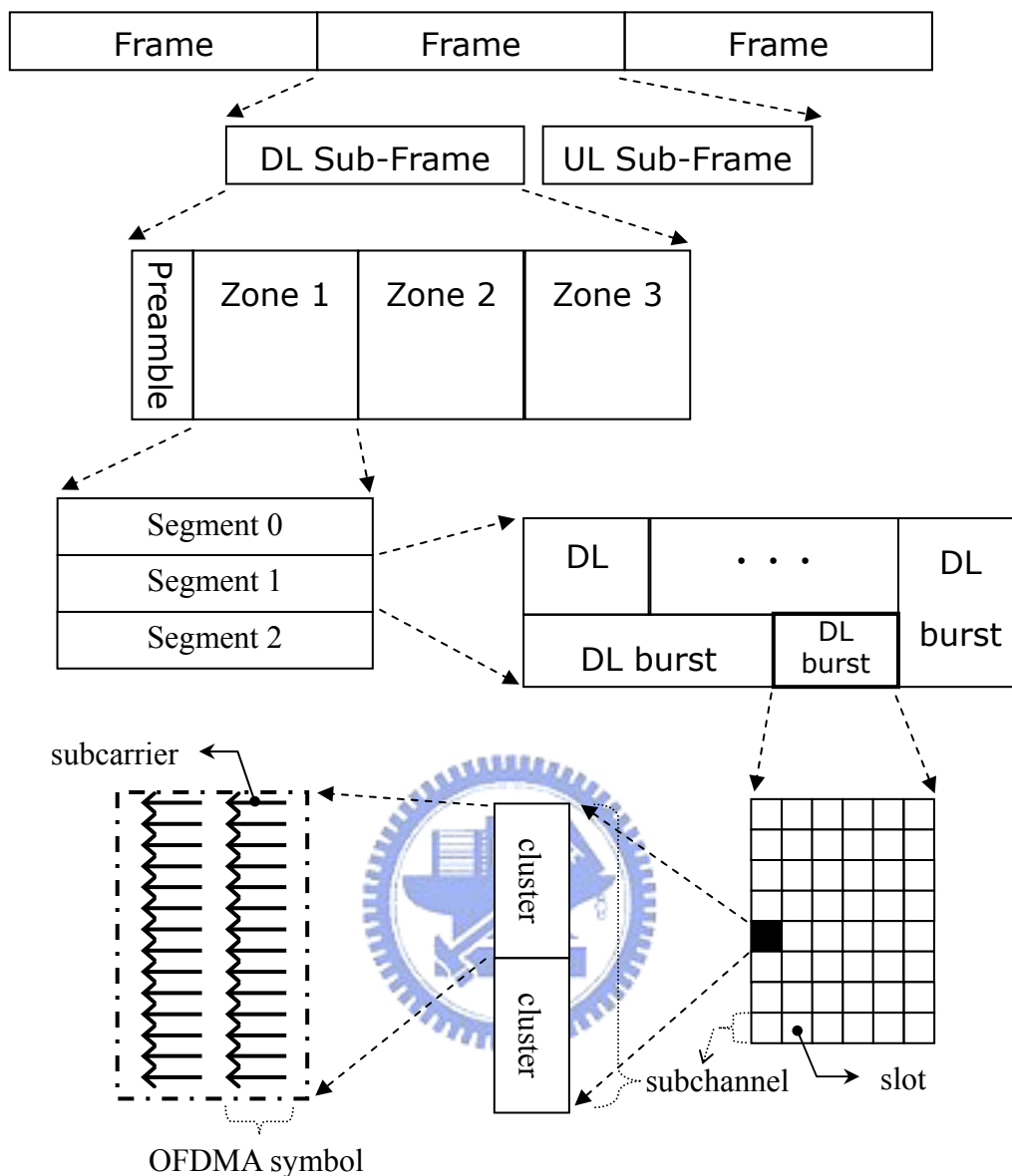
Figure 2-5 : OFDMA unit structure

2.1.4 Frame control section

The frame control section is the downlink burst following the preamble. It is used for control information

n destined for all subscriber stations (SSs). In OFDMA PHY, the frame control section contains a DL_Frame_Prefix, a DL-MAP message, and a UL-MAP message.

The DL_Frame_Prefix is a data structure transmitted at the beginning of each

frame and contains information regarding the current frame and is mapped to the frame control header (FCH). The information in DL_Frame_Prefix contains:

- Used subchannel bitmap: A bitmap indicates which groups of subchannel are used.
- Repetition coding indication: Indicates the repetition code used for the DL-MAP.
- Coding indication: Indicates the encoding code used for the DL-MAP.
- DL-MAP length: Defines the length of the DL-MAP message.

The first 4 slots in the downlink part of every segment contain FCH. These slots contain 48 bits modulated by QPSK with coding rate 1/2 and repetition coding of 4.

The DL-MAP of each segment should be mapped to the slots allocated to the segment in a frequency-first order, starting from the slot after the FCH. It contains various information element fields.

The UL-MAP message should immediately follow the DL-MAP message for uplink channel.

2.1.5 Baseband system

The baseband represents the whole physical layer except analog and RF parts. In the transmitter, the baseband system can be roughly divided into two modules:

- Channel coding
- Subcarriers allocation

In the receiver, it is mainly divided two modules: inner receiver and outer receiver. The outer receiver is further divided into the two modules as that in the transmitter. Inner receiver is a special module that does not have the corresponding counterpart in the transmitter. It uses preambles to perform timing and frequency synchronization.

Figure 2-6 illustrates the architecture of the baseband processing system.
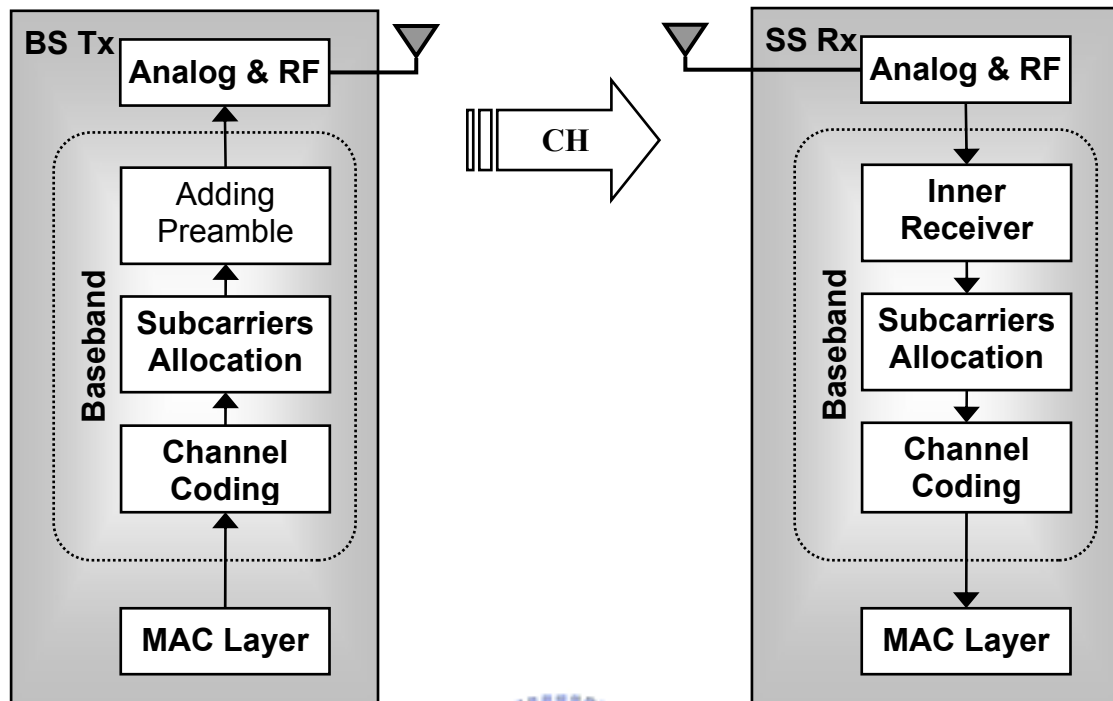
Figure 2-6 : Baseband communication system

The operations of the transmitter and the outer receiver will be discussed in this chapter. The operation of the inner receiver will be explained in the next chapter.

2.2 Channel Coding

Originally, channel coding indicates a forward error-correction coding (FEC) that can help data transmitted through noisy channel. Here, we extend its meaning to a procedure including other related operations. For example, it includes randomization, FEC encoding, bit interleaving, repetition and modulation, as shown in Figure 2-7. These functions will be explained later.

Figure 2-7 : Channel coding process

2.2.1 Concatenation

Concatenation is a function that divides one data burst into blocks. Each block is a basic unit for channel coding. There is a limit for the largest block size for an applied modulation and coding scheme. If the amount of MAC data to be transmitted does not fit exactly the amount of burst data allocated, 0xFF ("1" only) padding should be conducted to the end of the transmission block, up to the amount of data allocated. Table 2-1 gives the basic sizes of the useful data payloads per slot to be encoded in relation with the selected modulation type and coding rate. Table 2-2 and Table 2-3 show the rules used for concatenation.

	QPSK		16 QAM		64 QAM		
Coding rate	R=1/2	R=3/4	R=1/2	R=3/4	R=1/2	R=2/3	R=3/4
Data payload (bytes)	6	9	12	18	18	24	27

Table 2-1 : Data payload for a slot

Modulation and rate	j
QPSK 1/2	j=6
QPSK 3/4	j=4
16 QAM 1/2	j=3
16 QAM 3/4	j=2
64 QAM 1/2	j=2
64 QAM 2/3	j=1
64 QAM 3/4	j=1

Table 2-2 : Encoding subchannel concatenation

Number of slots	Slots concatenated
n≦j	1 block of n slots

n≧j	If (m=0)
	k blocks of j slots
	else
	(k-1) blocks of j slots
	1 block of ceil((m+j)/2) slots
	1 block of floor((m+j)/2) slots

Table 2-3 : Subchannel concatenation rule

The parameters used above are defined as:

- j: parameter dependent on the modulation and coding rate (see next figure)
- n: floor(number of allocated slots/repetition factor)
- k: floor(n/j)
- m: n modulo j

For example: let a burst have 1024 bytes, modulation be 16-QAM, coding rate be 1/2, and the code have no repetition. Then, the size of data payload is 12 bytes and j=3. Then, n=floor(ceil(1024/12)/1)=86, k=floor(86/3)=28, and m=86 mod 3=2. We can calculate that the burst is divided into 27 blocks of 3 slots, 1 block of 3 slots, and 1block of 2 slots.

2.2.2 Randomization

Randomization is a function that randomizes the data to prevent the constant ones or zeros that can decrease the performance of coding and modulation. Data randomization is performed on all data transmitted on the downlink and uplink, except those in the FCH. It is initialized on each FEC block.

The randomizer consists of a pseudo-random binary sequence (PRBS) generator and an XOR. The PRBS is generated with a shift feedback register having the function of $1+x^{14}+x^{15}$, as shown in Figure 2-8. Each data byte to be transmitted enters the randomizer sequentially, MSB first. The seed for the shift feedback register is used to generate the randomization bits, which are combined in an XOR operation with the serialized bit stream of each FEC block.
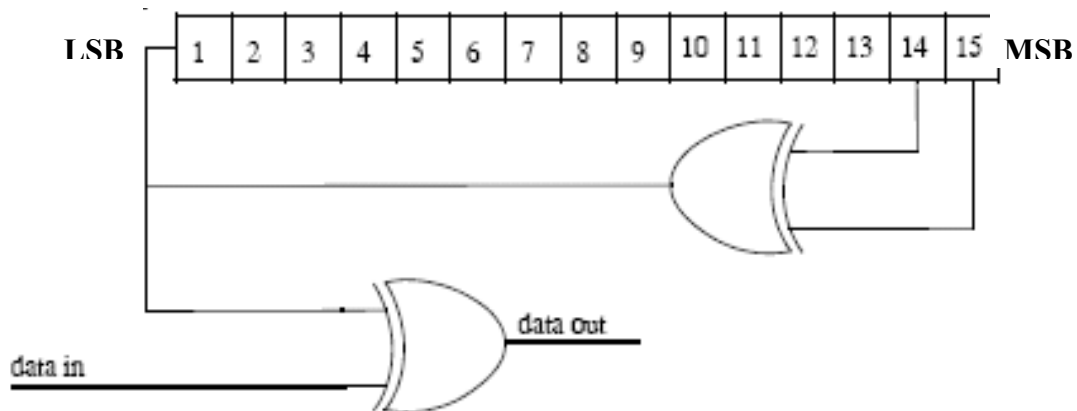
Figure 2-8 : PRBS for data randomization

The randomizer is initialized with the vector: [LSB] 0 1 1 0 1 1 1 0 0 0 1 0 1 0 1 [MSB].

2.2.3 Coding

The mandatory coding scheme is the tail-biting convolutional coding. Each FEC block is encoded by the binary convolutional encoder, which have native rate of 1/2, a constraint length equal to K=7. The following generator polynomials are used to derive its two coded bits:

$$G_1 = 171_{OCT} \quad \text{For } X$$
$$G_1 = 133_{OCT} \quad \text{For } Y$$

The generator is depicted in Figure 2-9.
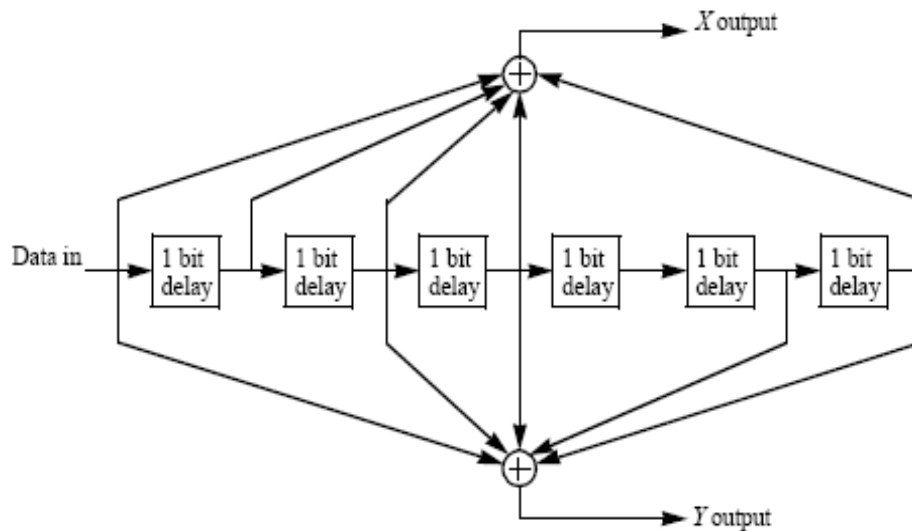
Figure 2-9 : Convolutional encoder of rate 1/2

Each block is encoded by a tail-biting convolutional encoder, which is achieved by initializing the encoder's memory with the last data bits of the FEC block being encoded.

The puncturing patterns and serialization order that is used to realize different code rates are defined in Table 2-4. In the figure, "1" means a transmitted bit and "0" denotes a removed bit, whereas X and Y can be referred to Figure 2-9.

Code Rates	1/2	2/3	3/4
d_{free}	10	6	5
X	1	10	101
Y	1	11	110
XY	X_1Y_1	$X_1Y_1Y_2$	$X_1Y_1Y_2X_3$

Table 2-4 : Puncture configuration

2.2.4 Bit-interleaving

The interleaver is defined by a two-step permutation operation. The first step ensures that adjacent coded bits are mapped onto nonadjacent subcarriers. The second

15

permutation insures that adjacent coded bits are mapped alternately onto the least or most significant bits of the constellation, thus avoiding long runs of lowly reliable bits.

(C) Interleaver

Let N_{cpc} be the number of coded bits per subcarrier, i.e., 2, 4, or 6 for QPSK, 16-QAM, or 64-QAM, respectively. Let $s=N_{cpc}/2$. Within a block of N_{cbps} (number of coded bits per symbol) bits at transmission, let k be the index of the coded bit before the first permutation, m_k be the index of that coded bit after the first and before the second permutation, j_k be the index after the second permutation, just prior to modulation mapping, and d be the modulo used for the permutation.

The first step permutation is defined as:

$$m_k = \left(N_{cbps}/d\right)\cdot k_{\mathrm{mod}(d)} + floor(k/d) \qquad k = 0,1,\cdots,N_{cbps}-1 \quad d = 16 \quad (2\text{-}1)$$

The second step permutation is defined as:

$$j_k = s\cdot floor(m_k/s) + \left(m_k + N_{cbps} - floor(d\cdot m_k/N_{cbps})\right)_{\mathrm{mod}(d)}$$
$$k = 0,1,\cdots,N_{cbps}-1 \quad d = 16 \qquad (2\text{-}2)$$

(D) De-interleaver

The de-interleaver, which performs the inverse operation of the interleaver, is also defined by two permutations. Within a received block of N_{cbps} bits, let j be the index of a received bit before the first permutation, m_j be the index of that bit after the first and before the second permutation, and k_j be the index after the second permutation, just prior to delivering the block to the decoder.

The first step permutation is defined as:

$$m_j = s \cdot floor(j/s) + \left(j + floor(d \cdot j / N_{cbps})\right)_{\mathrm{mod}(s)}$$
$$j = 0, 1, \cdots, N_{cbps} - 1 \quad d = 16 \tag{2-3}$$

The second step permutation is defined as:

$$k_j = d \cdot m_j - \left(N_{cbps} - 1\right) \cdot floor(d \cdot m_j / N_{cbps})$$
$$j = 0, 1, \cdots, N_{cbps} - 1 \quad d = 16 \tag{2-4}$$

2.2.5 Repetition

Repetition coding can be used to further increase signal margin over the original modulation and coding mechanisms. Let the repetition factor be R. For uplink, the allocated slots are repeated R times. For downlink, the number of the allocated slots is in the range of [R×K,R×K+(R−1)], where K is the number of the required slots before applying the repetition scheme. Here, R can be 2, 4, or 6. For example, when the required number of slots before the repetition is 10 (K=10) and the repetition factor R is 6, then the number of the allocated slots (Ns) for the burst can be from 60 slots to 65 slots.
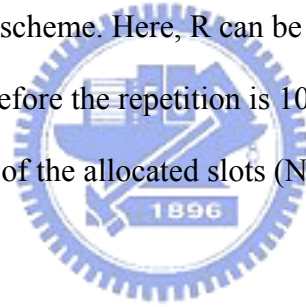
Thus, the binary data that fit into a region that is repetition coded is reduced by a factor R compared to an unrepeated region of the slots with the same size and FEC code type. After FEC and bit-interleaving, the data is partitioned into slots, and each group of bits designated to fit in a slot will be repeated R times to form R contiguous slots following the normal slot ordering that is used for data mapping.

2.2.6 Modulation

After repetition, the data bits then enter serially to the constellation mapper. Gray-mapped QPSK, 16-QAM, and 64-QAM are supported, as shown in Figure 2-10. Each M interleaved bits (M=2, 4, 6) are mapped to the constellation bits b(M-1)-b0 in MSB first order (i.e., the first bit should be mapped to the higher index bit in the

constellation), in addition, the M bits shall be ordered MSB first.
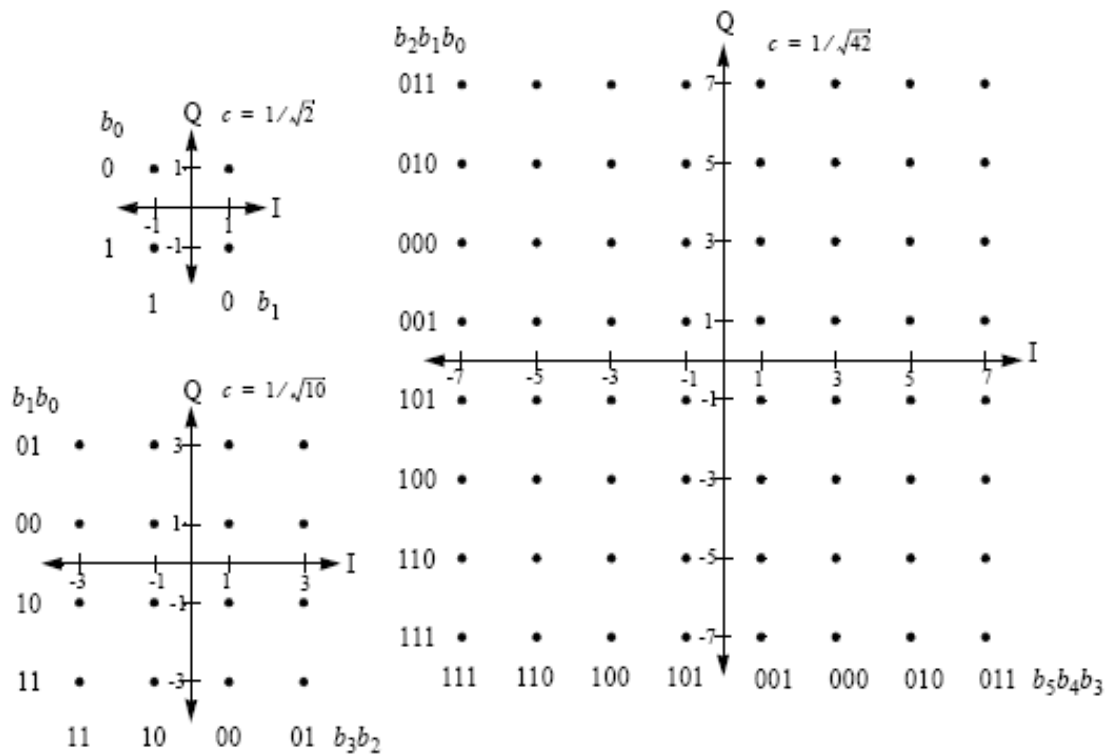
Figure 2-10 : Modulation constellations

2.3 Subcarrier Allocation

Subcarrier allocation can be performed according to following subcarrier usages: partial usage of subchannels (PUSC) and full usage of the subchannels (FUSC) in the downlink, PUSC in the uplink, and other optional usages. PUSC is corresponds to allocate some of the subchannels to the transmitter; FUSC to allocate all subchannels to the transmitter.

The OFDMA frame may include multiple zones include PUSC, FUSC, optional FUSC, and adaptive modulation and coding (AMC). In any case, the first zone must be the PUSC zone to ensure the successful receipt of DL_Frame_Prefix within the FCH and DL-MAP. This is because the SS does not have any message regarding allocation before first zone. Furthermore, the transition between zones is indicated in

the DL-MAP by the STC_LD_Zone. No DL-MAP or UL-MAP allocation can span

over multiple zones. Figure 2-11 depicts OFDMA frame with multiple zones.
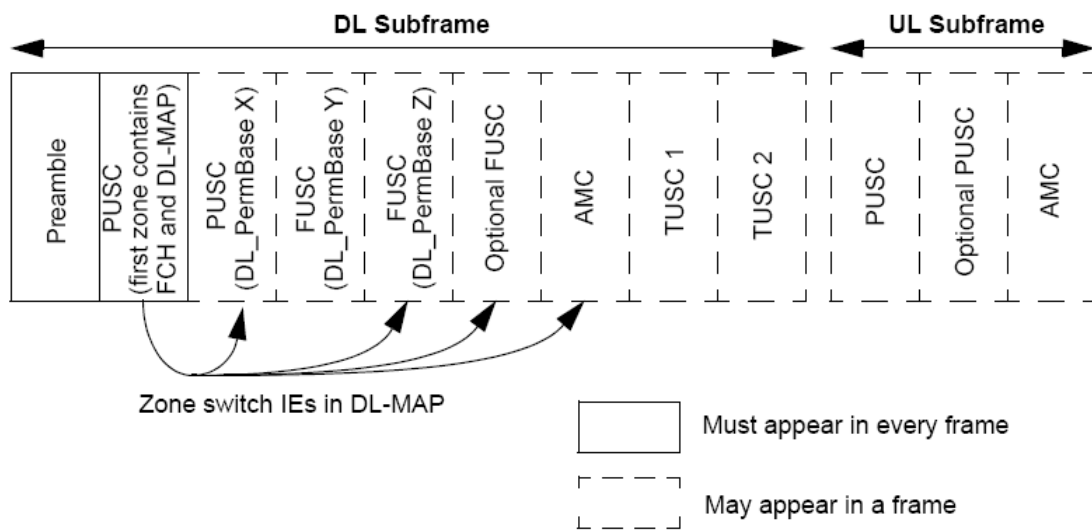
Figure 2-11 : Illustration of OFDMA frame with multiple zones

The downlink PUSC must appear in every frame. This thesis focuses on the subcarrier

allocation of DL-PUSC.

2.3.1 Introduction to DL PUSC

The symbol is first divided into basic clusters (half slot) and null carriers are

allocated. Then, pilots and data carriers are allocated within each cluster. Table 2-5

summarizes the parameters for DL PUSC.

Parameter	Value	Comments
Number of DC subcarriers	1	Index 1024 (counting form 0)
Number of Guard subcarriers, Left	184	
Number of Guard subcarriers, Right	183	
Number of used subcarriers	1681	Number of all subcarriers used within a

(N$_{used}$)		symbol, including all possible allocated pilots and the DC carrier.
Number of subcarriers per cluster	14	
Number of cluster	120	
Renumbering sequence	1	Used to renumber clusters before allocation to subchannels: 6,108,37,81,31,100,42,116,32,107,30,93,54,78,10,75,50,111,58,106,23,105,16,117,39,95,7,115,25,119,53,71,22,98,28,79,17,63,27,72,29,86,5,101,49,104,9,68,1,73,36,74,43,62,20,84,52,64,34,60,66,48,97,21,91,40,102,56,92,47,90,33,114,18,70,15,110,51,118,46,83,45,76,57,99,35,67,55,85,59,113,11,82,38,88,19,77,3,87,12,89,26,65,41,109,44,69,8,61,13,96,14,103,2,80,24,112,4,94,0
Number of data subcarriers in each symbol per subchannel	24	
Number of subchannels	60	
Basic permutation sequence 12 (for 12 subchannels)		6,9,4,8,10,11,5,2,7,3,1,0
Basic permutation sequence 8 (for 12 subchannels)	4	7,4,0,2,1,5,3,6

Table 2-5 : OFDMA downlink carrier allocations-PUSC

Figure 2-12 shows the partition from a frame to a subcarrier in frequency domain. One frame of used subcarriers (1680 subcarriers excluding DC) is divided into three segments, each segment of 560 subcarriers is divided into 20 subchannels, each subchannel of 28 subcarriers is divided into two clusters, and each cluster (14 subcarriers) is divided into 12 data subcarriers and 2 pilot subcarriers. The location of the pilot subcarrier is also depicted in the figure. Note that the slot and the cluster are two-dimensional, and one cluster corresponds to exactly a half slot.
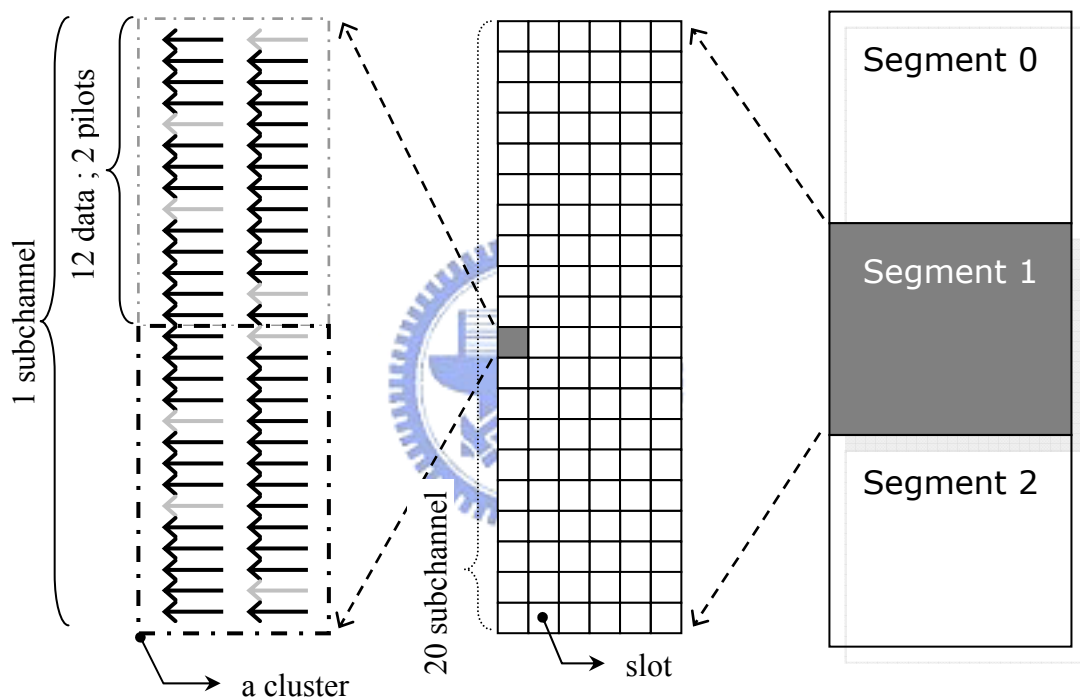
Figure 2-12 : Partition for PUSC units

2.3.2 Data Mapping

After modulation, the constellation-mapped data are subsequently allocated onto slots and then to the burst area (OFDMA data region). The subcarrier allocation within a slot uses the algorithms described below, as also depicted in Figure 2-13.

- Modulated data shall span continuous 24 data subcarriers and two consecutive OFDMA symbols. Map the data such that the lowest numbered QAM symbol

21

maps to the lowest numbered subcarrier and the lowest numbered OFDM
symbol.

● Continue the mapping such that the subcarrier index is increased. When the
edge of the slot is reached, continue the mapping from the lowest numbered
subcarrier in the next available OFDMA symbol.
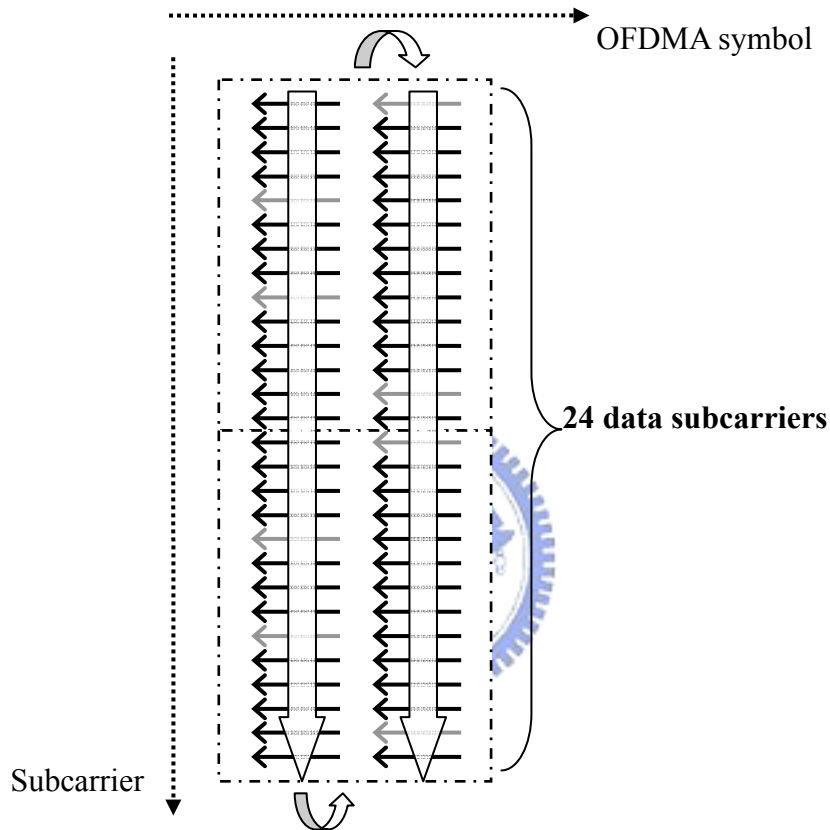
Figure 2-13 : Mapping subcarriers to a slot

The slots allocation within a burst uses the algorithms described below, and also
depicted in Figure 2-14.

● Each slot shall span one subchannel and two OFDMA symbols. Map the slots
such that the lowest numbered slot occupies the lowest numbered subchannel
in the lowest numbered OFDMA symbol.

● Continue the mapping such that the OFDMA subchannel index is increased.
When the edge of the burst is reached, continue the mapping from the lowest

numbered subchannel in the next available OFDMA symbol.
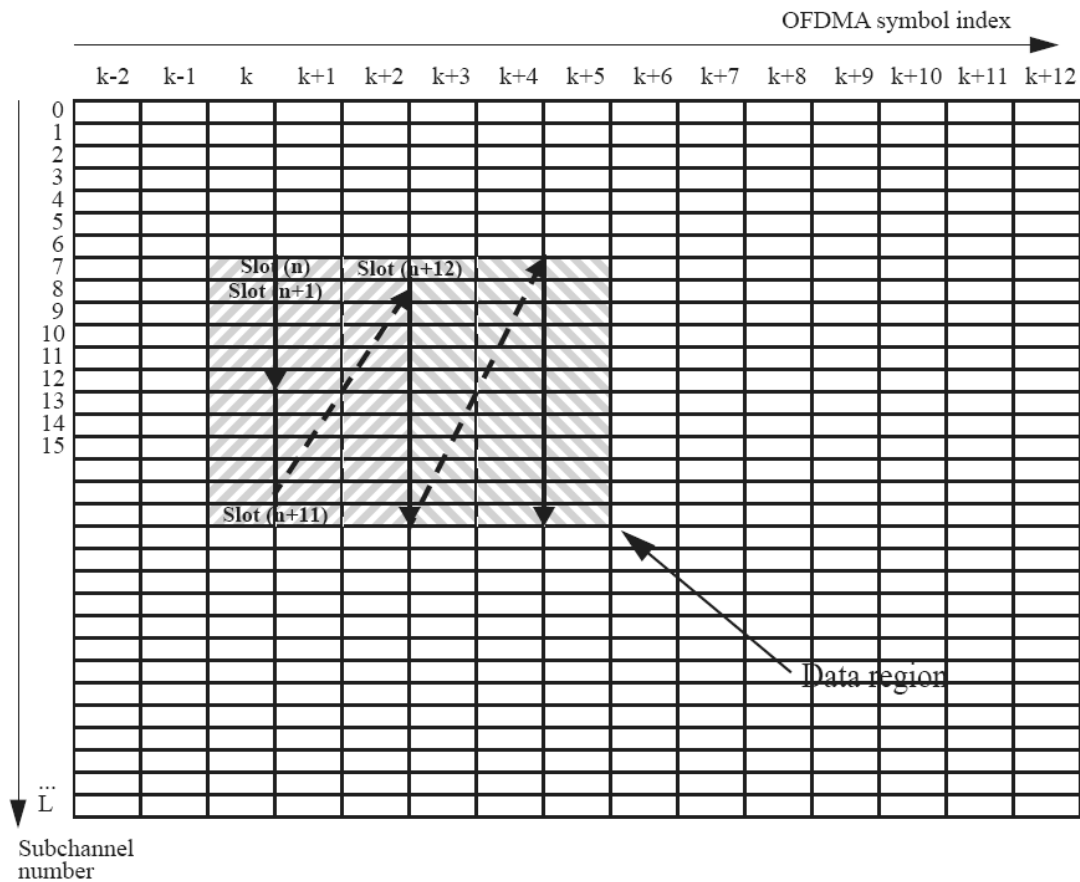
Figure 2-14 : Mapping slots to a burst

2.3.3 Permutation

The permutation is a function similar to the subcarrier interleaving. It exchanges the location of subcarriers to resist frequency-selected channel fading.

One segment is divided into one big group of 12 subchannels and another small group of 8 subchannels. The number of subchannels per group is denoted $N_{subchannels}$ and the number of subcarriers per subchannel is denoted $N_{subcarriers}$. As mentioned, one subchannel contains 24 data subcarriers in PUSC. Then, allocating subcarriers in each group to subchannels for each OFDMA symbol using (2-5), called a permutation formula.

$$subcarrier(k, s)$$
$$= N_{subchannels} \cdot n_k + \{p_s[n_k \bmod N_{subchannels}] + DL\_PermBase\} \bmod N_{subchannels} \tag{2-5}$$

where

$subcarrier(k, s)$ is the subcarrier index of subcarrier k in subchannel s,

k is the subcarrier-in-subchannel index form the set

$[0 \ldots N_{subcarriers} - 1]$,

s is the index number of a subchannel, from the set

$[0 \ldots N_{subchannels} - 1]$,

n_k $= (k + 13 \cdot s) \bmod N_{subcarriers}$

$N_{subchannels}$ is the number of subchannels, 12 in even group and 8 in odd

group

$N_{subcarriers}$ is the number of data subcarriers per subchannel in each

OFDMA symbol,

$p_s[j]$ is the series obtained by rotating basic permutation sequence

cyclically to the left s times,

DL_PermBase   is an integer ranging from 0 to 31, which is set to preamble

IDcell in the first zone and determined by the DL-MAP for

other zones

On initialization, an SS must search for the downlink preamble. After finding the preamble, the SS will know the IDcell used for permutation. For example, if IDcell in received preamble is "2", the even group permutation is performed as that in Figure 2-15.
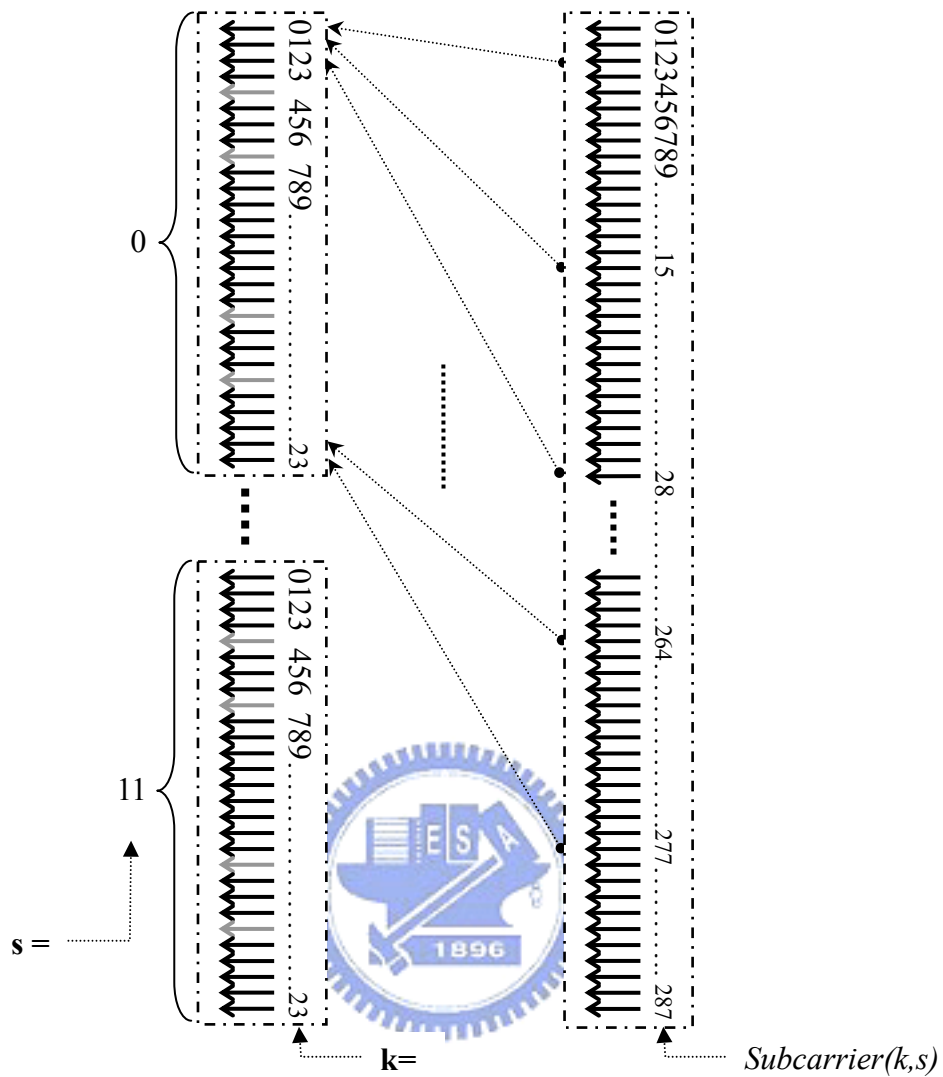
Figure 2-15 : Permutation concept

2.3.4 Renumbering

Since PUSC subcarrier permutation is conducted in each group separately, subcarriers will not be exchanged among groups. The function of the renumbering is to interleave subcarriers among groups. The operation is described below, and also depicted in Figure 2-16.

Renumbering uses a cluster as the basic unit to exchange the logical clusters into physical clusters using (2-6):

LogicalCluster

$$= \begin{cases} RenumberingSequence(PhysicalCluster) & \text{First DL zone, or SC indicator} = 0 \\ & \text{in STC\_DL\_Zone\_IE} \\ RenumberingSequence((PhysicalCluster + 13 \times DL\_PermBase) \bmod 120) & \text{otherwise} \end{cases}$$

(2-6)

For example, the 2nd (from 0) physical cluster is derived from the 37th logical cluster.
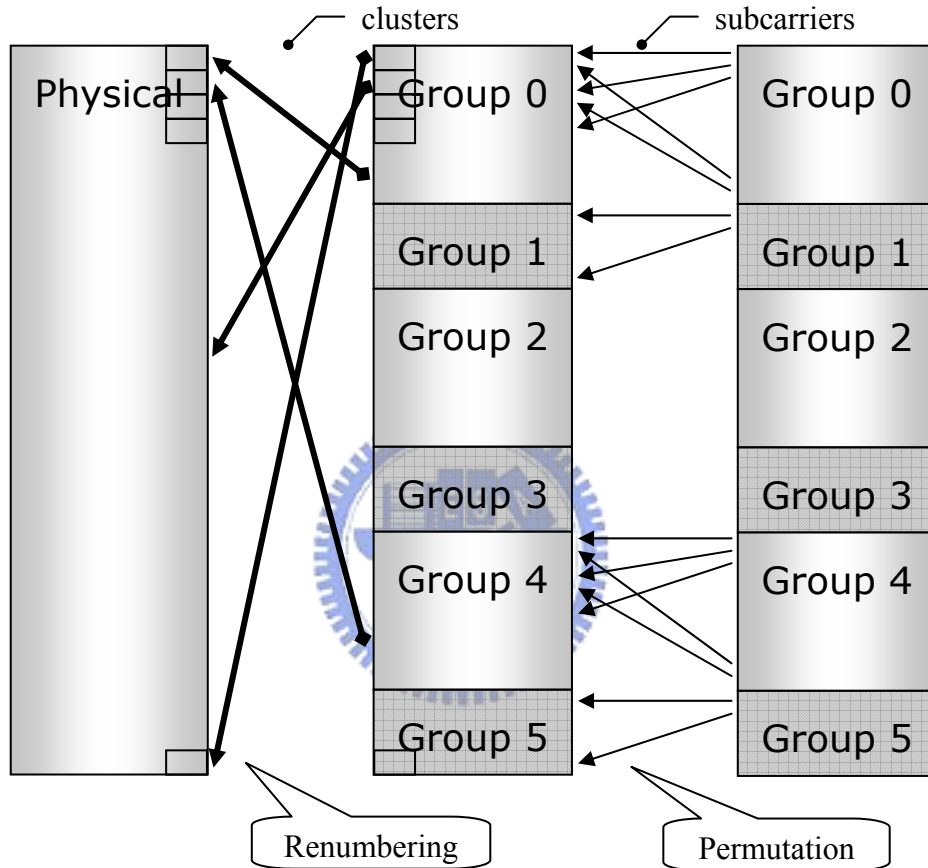
Figure 2-16 : Renumbering concept

2.3.5 Pilot and Subcarrier Randomization

Pilots, similar to the preamble, are known by the receiver before data transmission. They are inserted into data sequence instead of the beginning of the frame. The receiver can use pilots for synchronization and channel estimation. In PUSC, the pilots are inserted with a regular pattern in a cluster. For the even OFDMA symbol (including first symbol just after preamble), pilots are located on 4th and 8th

(from 0) subcarriers in a cluster, and for the odd symbol, they are located on 0th and 12th subcarriers in a cluster.

The subcarrier randomization is different from the data randomization. The value of pilots and that of subcarrier randomization are generated to the same PRBS sequence. They use the same PRBS generator to modulate pilot signals and the randomization sequence. The subcarriers will be multiplied by the sequence to randomize the subcarriers. The PRBS generator depicted in Figure 2-17 should be used to produce a sequence, 'w_k', where 'k' is physical (after renumbering) used subcarrier index. The polynomial for the generator is '$X^{11}+X^9+1$'.

Figure 2-17 : PRBS generator for pilot modulation and subcarrier randomization

The initialization vector of the PRBS generator for both uplink and downlink is designated as b10~b0, such that:

- b0~b4 = Five least significant bits of IDcell as indicated by the frame preamble in the first downlink zone and in the downlink AAS zone with

27

Diversity_Map support, DL_PermBase following STC_DL_Zone_IE, and 5

LSB of DL_PermBase following AAS_DL_IE without Diversity_Map support

in the downlink. Five least significant bits of IDcell (as determined by the

preamble) in the uplink. For downlink and uplink, b0 is MSB and b4 is LSB,

respectively.

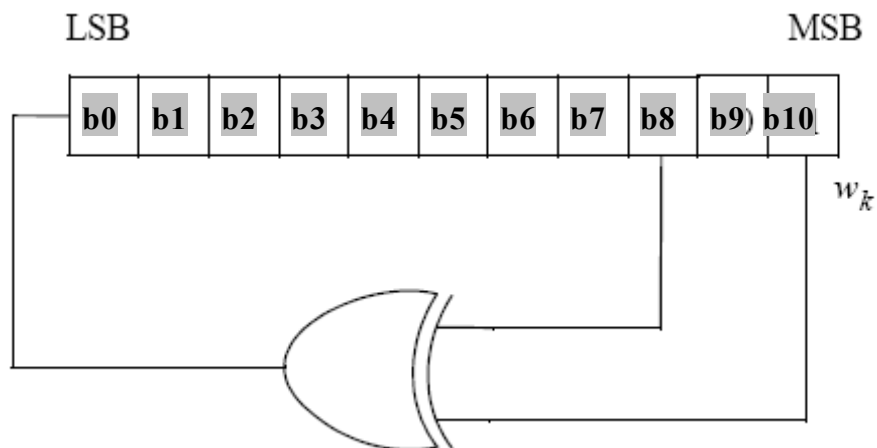- b5~b6 = Set to the segment number + 1 as indicated by the frame preamble in

  the first downlink zone and in the downlink AAS zone with Diversity_Map

  support, PRBS_ID as indicated by the STC_DL_Zone_IE or AAS_DL_IE

  without Diversity_Map support in other downlink zones, and 0b11 in the

  uplink. For downlink and uplink, b5 is MSB and b6 is LSB, respectively.

- b7~b0 =0b1111 (all ones) in the downlink and four least significant bits of the

  Frame Number in the uplink. For downlink and uplink, b7 is MSB and b10 is

  LSB, respectively.

For example, the initialization vector of the PRBS generator is b10~b0 =

10101010101, the result in the sequence w_k = 1010101010100000… in the

uplink.

A new value is generated by the PRBS generator for every subcarrier up to the

highest numbered usable subcarrier, in the order of physical subcarriers, including the

DC subcarrier and usable subcarriers that are not allocated. Furthermore, The PRBS

generator should be clocked "n+N_{used}-1" times, n is equal to symbol offset mod 32

and N_{used} is the number of used subcarriers, where symbol offset is counted from the

first symbol in each zone. This is because the beginning of the PRBS sequence of the

symbol would be shifted by its symbol offset. Consider DL PUSC, let w0,w1,w2,…

be the bits generated after the initialization. The subcarriers of the first symbol in the

zone (with symbol offset of zero) use the bits w0,w1,w2,…,w1680. For the second

symbol (with symbol offset of 1) use the bits w1,w2,w3,…,w1681. Thus, if there are

30 symbols in first PUSC zone, the PRBS generator should be clocked

"30+1681-1=1710" times.

After generating w_k, the pilot subcarrier c_k should be modulated according to

following equations.

- For the mandatory tile structure in the uplink, and for the other allocations

  such as TUSC1/TUSC2 structures in the downlink:

$$\mathrm{Re}\{c_k\} = 2\left(\frac{1}{2} - w_k\right)$$
$$\mathrm{Im}\{c_k\} = 0$$

(2-7)

- In all permutations except uplink PUSC and downlink TUSC1, each pilot shall

  be transmitted with a power boosted of 2.5 dB higher than the average

  non-boosted power of each data tone:

$$\mathrm{Re}\{c_k\} = \frac{8}{3}\left(\frac{1}{2} - w_k\right) \cdot p_k$$
$$\mathrm{Im}\{c_k\} = 0$$

(2-8)

Where p_k is the pilot's polarity for spatial division multiple access (SDMA)

allocations in AMC AAS zone, and $p = 1$ otherwise.

The subcarrier randomization is accomplished as each modulated data subcarrier

is multiplied by the factor $2\left(\frac{1}{2} - w_k\right)$. In DL PUSC, we can combine the pilot and

randomization by inserting the value of 4/3 into pilot subcarriers and then multiplying

both pilot and data subcarriers with the same factor $2\left(\frac{1}{2} - w_k\right)$.

2.4 Summary

Figure 2-18 illustrates the OFDMA PHY transmitter architecture in DL PUSC.

The channel coding includes concatenation, data randomization, convolutional

encoding, bit-interleaving, repetition encoding, and modulation. The subcarrier

allocation includes data mapping, permutation, renumbering, pilot insertion, and

subcarrier randomization. Then, passing the resultant signal through IFFT and adding

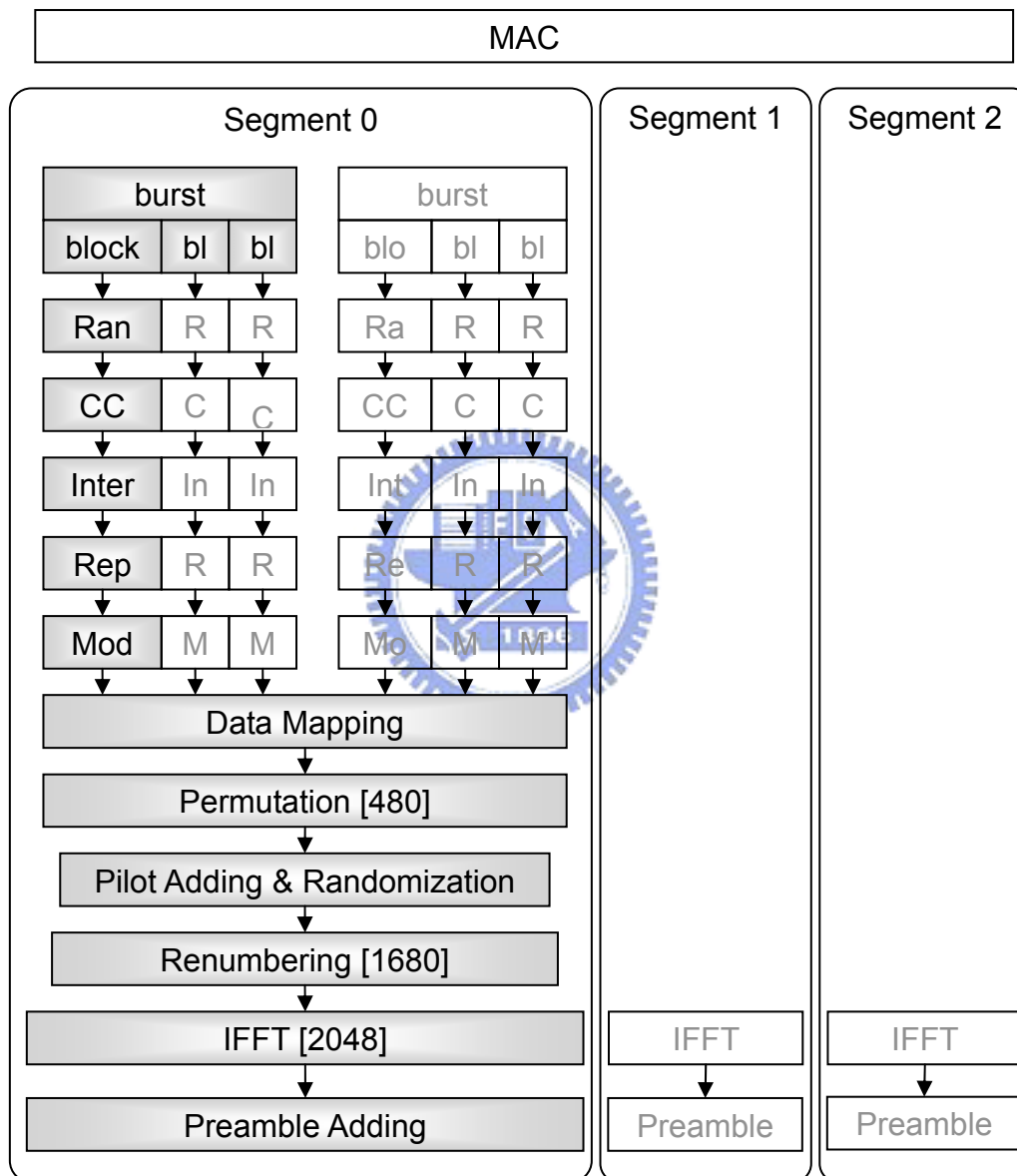preamble, we can complete the whole baseband processing for transmission.

Figure 2-18 : Baseband transmitter

Figure 2-19 illustrates the OFDMA PHY receiver architecture in DL PUSC. It

consists of an inner and outer receiver. The outer receiver reverses the operation

conducted in the transmitter, while the inner receiver performs synchronization,

channel estimation, and equalization.
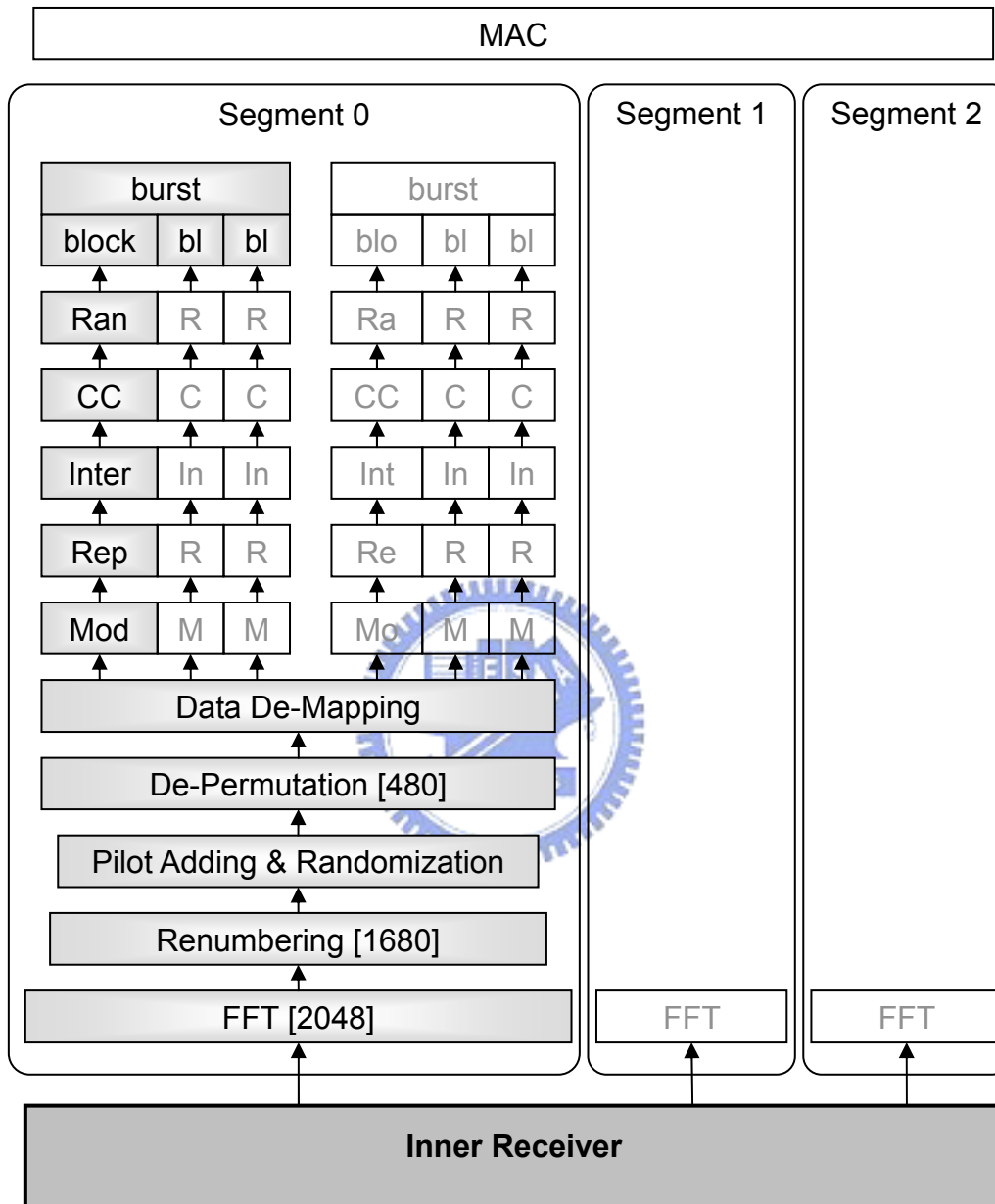
Figure 2-19 : Baseband receiver

Chapter 3: Synchronization

3.1 Preamble Structure

The preamble, having a specific pattern and containing symbols known to the receiver, is usually used for synchronization. Here synchronization is defined in a broader sense, which includes packet detection, frequency offset estimation, timing offset estimation, and channel estimation. The length and contents of the preamble are specially designed such that information for synchronization is just enough avoiding any unnecessary overhead.

3.1.1 Frequency Domain Data

As mentioned, the thesis focuses on the FFT size of 2048 (IEEE 802.16-2004). The data transmitted in the preamble are defined in the frequency domain. Equation (3-1) shows subcarrier allocation for the preamble data, which is modulated with a boosted BPSK modulation scheme with a specific pseudo-noise (PN) code described below.

$$PreambleCarrierSet_n = n + 3 \cdot k \qquad (3\text{-}1)$$

where

$PreambleCarrierSet_n$ specifies all subcarriers allocated to the specific
preamble

N in the number of the preamble carrier-set indexed 0~2

K is a running index 0~567

Each segment uses one type of preamble out of three sets:

- Segment 0 uses preamble carrier-set 0

- Segment 1 uses preamble carrier-set 1

- Segment 2 uses preamble carrier-set 2

Thus, each segment eventually use one third of subcarriers for preamble transmission. In the case of segment 0, the DC carrier will not be used and the corresponding PN will be discarded. In other words, DC carrier should always be zeroed. For the preamble symbol, there will be 172 guard band subcarriers on the left and right sides of its used spectrum. Figure 3-1 illustrates the distribution of three carrier-sets.
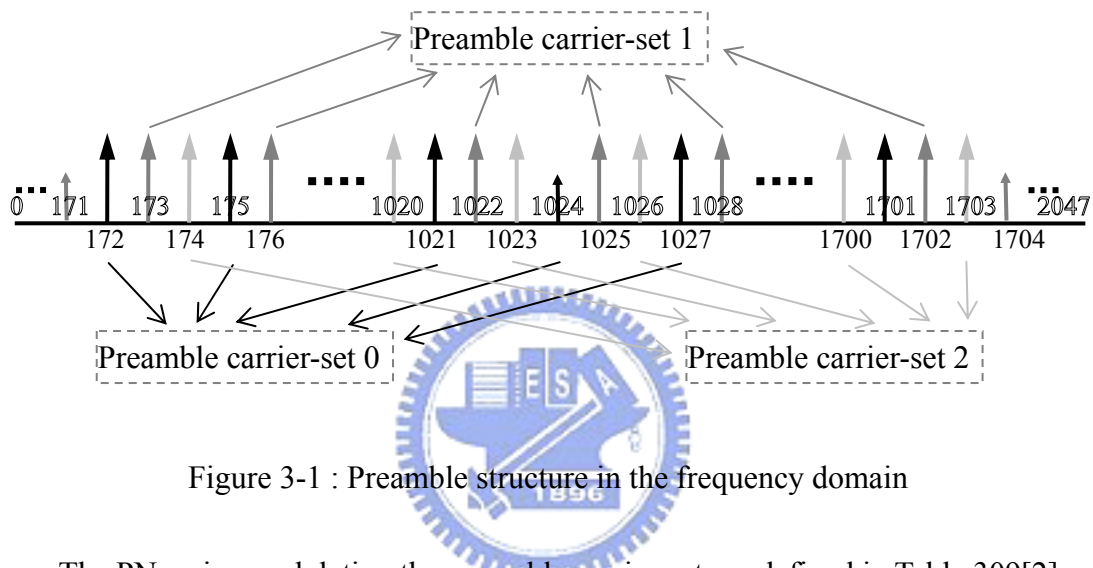
Figure 3-1 : Preamble structure in the frequency domain

The PN series modulating the preamble carrier-set are defined in Table 309[2] [3] . Note that the preamble series table includes PN sequence in a Hexadecimal format. In PUSC, there are total 114 preamble series; the actual series used depends on the designated segment and the IDcell parameter. Each segment can have 38 different preamble series. The series specified is mapped onto the preamble subcarriers in ascending order. The PN series is converted into to a binary series (w_k) with values of plus and minus one (0 mapped to +1 and 1 mapped to -1).

3.1.2 Time Domain Waveform

Once the preamble data in the frequency domain are defined, the preamble waveform in the time domain can be obtained with IFFT. Since subcarriers allocated for the preamble series corresponds to a downsampled version of available subcarriers

(the downsampling factor is three), the time-domain preamble waveform is periodic

(three periods in the preamble), as depicted in Figure 3-2.
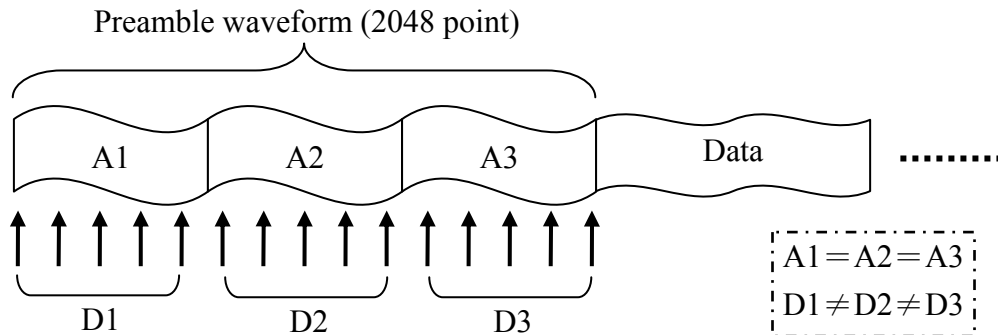
Figure 3-2 : Preamble structure in time domain

Note that the preamble is not exactly periodic. This is because the IFFT size is

2048, which is not divisible by three. In other words, the preamble contains three

signal sections, which are similar but not exactly the same. Even though, the

periodic property of the preamble can still be used for the purpose of

synchronization.
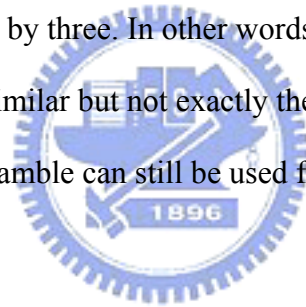
3.2 Channel Model

The channel between BS and SS can be roughly divided into two types. The first

one is the actual signal propagation channel. In wireless systems, this corresponds to

the mulipath fading channel, and the packet timing offset. The second one is the

non-ideal effect of analog and RF components, which will introduce distortions into

the received signal. The channel model we used is a combination of these two channel

effects. For the second type of channel effect, we consider the sampling timing offset

and the carrier frequency offset. Solutions have been developed to cope with these

effects and will be described in next section.

3.2.1 Multipath Fading Channel

Multipath fading occurs when the transmitted signal arrives at the receiver via multiple propagation paths having different delays and different intensities. These signal components may add destructively or constructively in the receiver. Note that the multipath channel will extend the transmitted signal period, as shown in Figure 3-3, which may result in inter-symbol interference (ISI) in the OFDM system. The received signal can be described in the time domain as:

$$r[n] = \sum_i h_i[n] \cdot s[n - \tau_i] + w[n] \qquad (3\text{-}2)$$

$$r = \mathbf{h} * s + n \qquad (3\text{-}3)$$

where r is received signal, h is channel impulse response, s is transmitted signal, w is AWGN, i is path index, and n is sample index. In the frequency domain, the received signal can be written as:

$$R[k] = H[k] \cdot S[k] + W[k] \qquad (3\text{-}4)$$

where $R[k]$ is the received frequency-domain signal, $H[k]$ is the channel frequency response, $S[k]$ is the transmitted frequency-domain signal, and $W[k]$ is AWGN, all for subcarrier k.
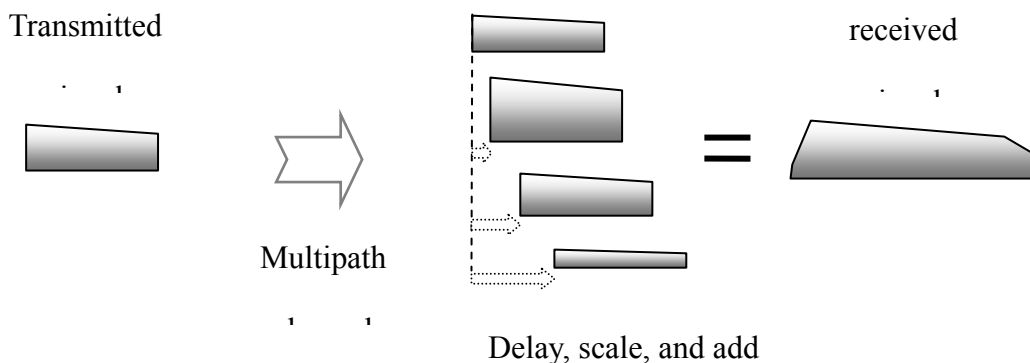

Figure 3-3 : Multipath fading effect

IEEE 802.16 task force does not specify channel models for simulations. We then use the spatial channel model (SCM) provided by the 3GPP. The channel environment of 3G systems, defined for wireless metropolitan area, is similar to that of 802.16. The SCM channel model can support fixed and mobile wireless multipath fading channels. Three different types of models are defined:

- Suburban macro-cell: The cell coverage is 1~6 Km. The BS antennas are set above rooftop height, ranging from 10m to 80 m. The average height is 32 m. The SS's mobile speed is between 0~250 Km/hr.

- Urban macro-cell: The cell coverage is 1~6 Km. The BS antennas are above rooftop height, their height is 10~80 m, and the average height is 32 m. The SS's speed is 0~250 Km/hr. Note that these settings are the same as those in suburban macro-cell; others may be different.

- Urban micro-cell (approximately 1Km distance from BS to BS): The cell coverage is 0.3~0.5 Km. The BS antennas are set at rooftop height; the average height is 12.5 m. The SS's speed is between 0~120 Km/hr.

3.2.2 Timing Offset

In the actual operation, the receiver cannot know when the packet will arrive. Thus, it has to perform some kind of detection. After that, the receiver has to synchronize the received symbol boundary. Timing offset also called "symbol offset" results from imperfect timing synchronization. The more accurate the timing synchronization is, the smaller the timing offset will be.

Assuming that the timing offset for the receiver is delayed by n_ε samples, which is equal to the actual sample n minus inaccuracy sample m ($n_\varepsilon = n - m$). The received samples as shown in (3-2) can be expressed as

$$r[m] = r[n - n_\varepsilon] = \sum_i h_i[n - n_\varepsilon] \cdot s[n - n_\varepsilon - \tau_i] + w[n - n_\varepsilon] \qquad (3\text{-}5)$$

Thus, we have the received signal in the frequency domain as

$$R'[k] = (H[k] \cdot S[k] + W[k]) \cdot e^{-j2\pi(k/N) \cdot n_\varepsilon} \qquad \text{where N is FFT size} \qquad (3\text{-}6)$$

From (3-6), we can see that the timing offset causes the phase rotation of the received signal (proportional to subcarrier index). In the no multipath fading condition, if the timing offset n_ε is larger than zero or smaller than the negative CP length, the inter-symbol interference (ISI) and inter-carrier interference (ICI) will occur, as depicted in Figure 3-4. Certainly, the multipath channel effect will extend the symbol length so that the toleration of timing offset becomes smaller.
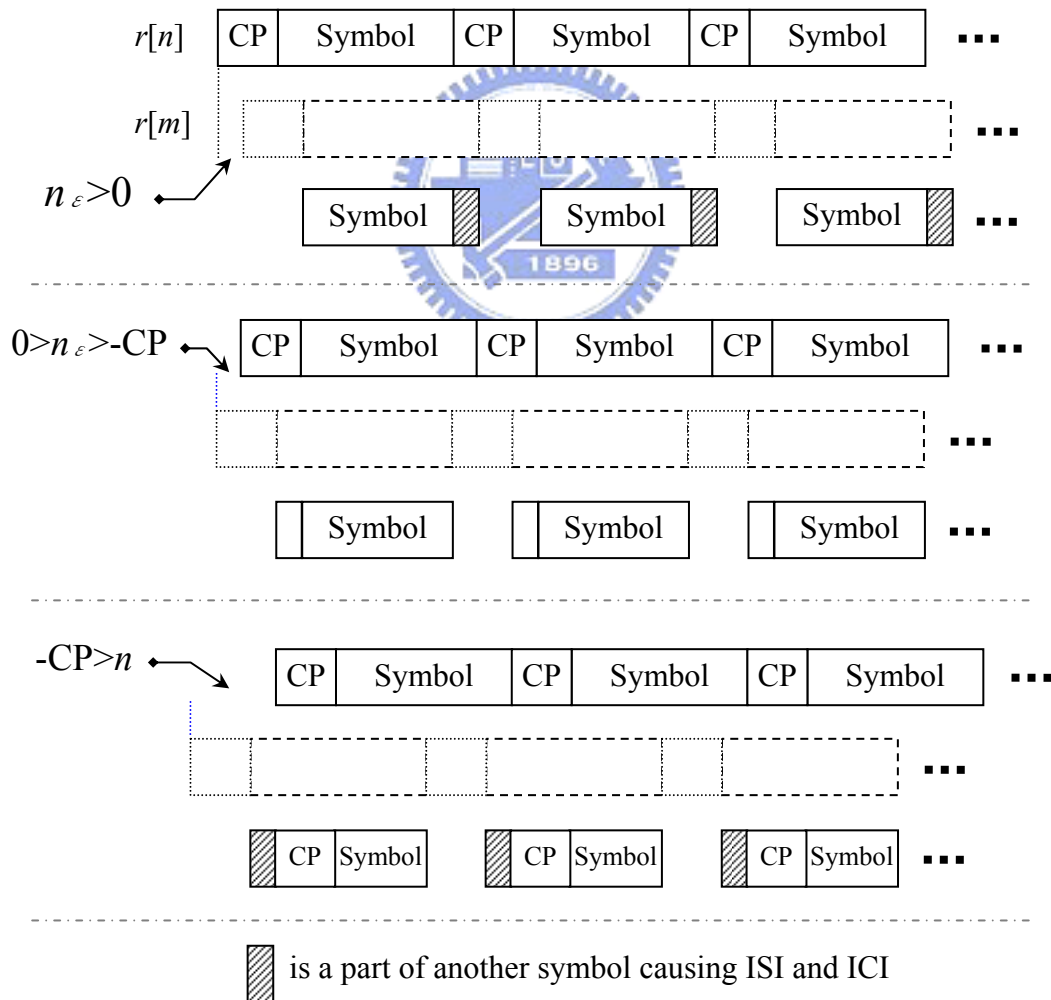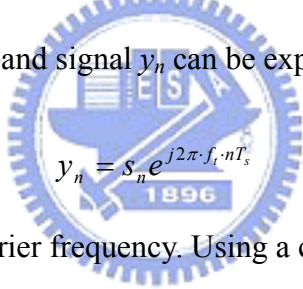

Figure 3-4 : ISI caused by timing offset

37

3.2.3 Frequency Offset

Both the transmitter and the receiver use their own oscillators to generate carrier and sampling signals. However, the signal generated from the oscillator in the receiver will never have the exact frequency as that from the transmitter. The difference between the transmitter and receiver oscillator frequencies is called frequency offset. The frequency offset can be divided into two types: The carrier frequency and sampling frequency offsets.

The carrier frequency offset (CFO) results from the mismatch between carrier frequencies. The OFDM systems use smaller subcarrier bandwidth so that they are more sensitive to CFO than single-carrier systems. Fortunately, large CFO can be corrected; only small residual CFO needs to be considered. Let the transmitted signal be s_n. Then, the complex passband signal y_n can be expressed as

$$y_n = s_n e^{j2\pi \cdot f_t \cdot nT_s} \tag{3-7}$$

where f_t is the transmitter carrier frequency. Using a carrier with frequency f_r, we can down-convert the received signal. Let the resultant baseband signal be r_n, we than have (ignoring noise for the moment)

$$
\begin{aligned}
r_n &= y_n \cdot e^{-j2\pi \cdot f_r \cdot nT_s} \\
&= s_n e^{j2\pi \cdot f_t \cdot nT_s} \cdot e^{-j2\pi \cdot f_r \cdot nT_s} \\
&= s_n e^{j2\pi \cdot (f_t - f_r) \cdot nT_s} \\
&= s_n e^{j2\pi \cdot f_\Delta \cdot nT_s}
\end{aligned}
\tag{3-8}
$$

where $f_\Delta = f_t - f_r$ is the frequency offset.

The sampling frequency offset (SFO) results from the mismatch between the frequency of the digital to analog converter (DAC) at the transmitter, and that of the analog to digital converter (ADC) at the receiver. The SFO will have two main effects: (1) a slow drift of the symbol timing boundary, which rotates the phase of the

subcarriers similar to timing offset, and (2) loss of the orthogonality of the subcarriers. This is due to the subcarriers are not sampled at the optimum positions and ICI will occur. This will also result in loss of signal to noise ratio (SNR)

Let the SFO be $\Delta T = T' - T$ where T' and T are the receiver and transmitter sampling periods, respectively, as shown in Figure 3-5. Then the normalized sampling error can be defined as $t_\Delta = \dfrac{T' - T}{T}$. After DFT, the received signal can be expressed as

$$R_l[k] = e^{j2\pi \cdot k \cdot t_\Delta \cdot l \frac{T_s}{T_u}} S_l[k] \cdot \operatorname{sinc}(\pi \cdot k \cdot t_\Delta) H_l[k] + W_l[k] + C(t_\Delta)_l[k] \quad (3\text{-}9)$$

where l is the OFDMA symbol index, k is the subcarrier index, T_s is the duration of the total symbol, T_u is the duration of the useful data portion, W_l is AWGN and $C(t_\Delta)_l$ is the induced ICI due to the SFO.
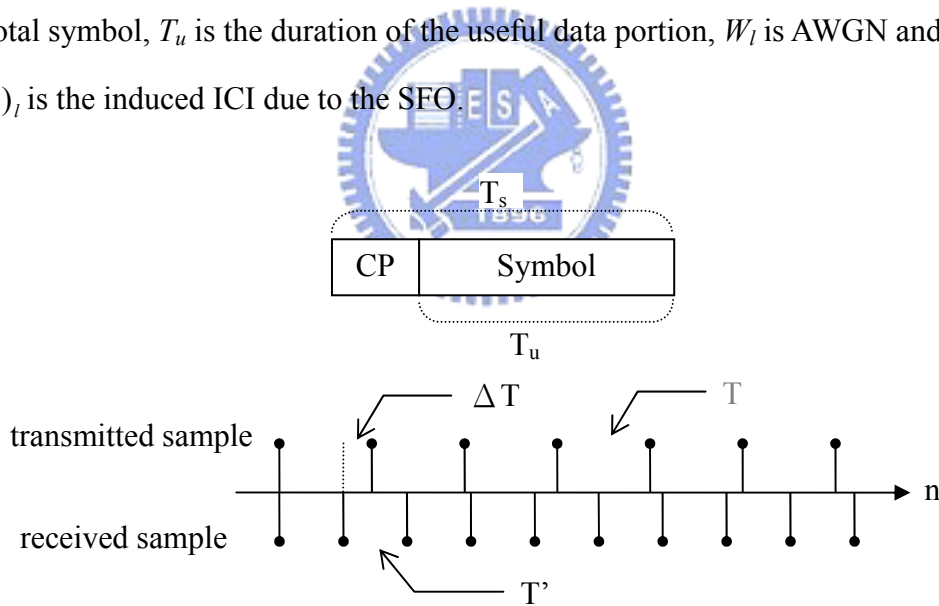
Figure 3-5 : Sampling frequency offset in the time domain

If the ΔT is small enough that the ICI term can be ignored, the remained significant term is $e^{j2\pi \cdot k \cdot t_\Delta \cdot l \frac{T_s}{T_u}}$. This term shows the amount of angle rotation experienced by the different subcarriers, as shown in Figure 3-6. The angle depends on both the subcarrier index k and the OFDMA symbol index l. Even though the term

ΔT is quite small, as *l* increases, the rotation may eventually become so large that correct demodulation is no longer possible. This is shown in Figure 3-7.

Figure 3-6 : Sampling frequency offset in the frequency domain

Figure 3-7 : Angle rotation increase by subcarriers and symbols

3.3 Synchronization Algorithms

Synchronized algorithms performed by the inner receiver will have great influence on the system performance. This is because most operations of the outer

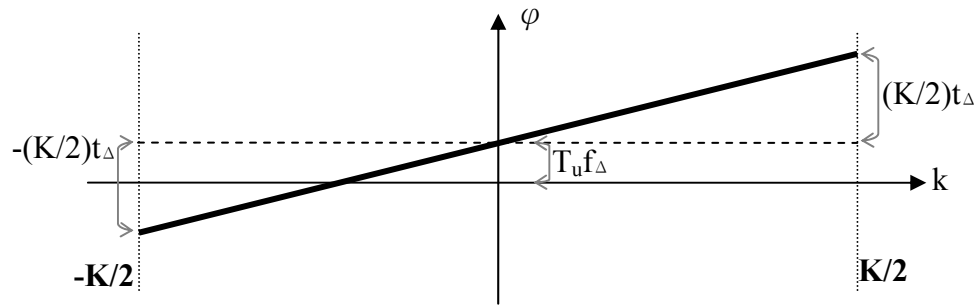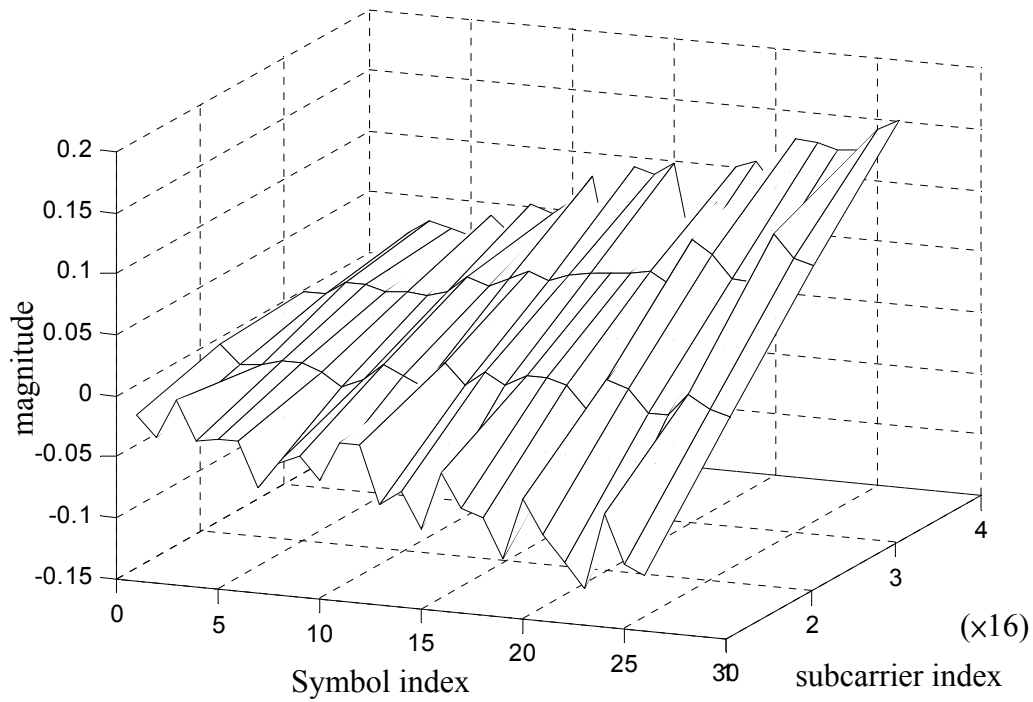receiver are already determined by the specification. Generally, synchronization includes several sub-functions such as: packet detection, DC offset compensation, automatic gain control, frequency synchronization, symbol timing correction, channel estimation, and phase tracking. Different from single-carrier systems, the OFDM system is sensitive to timing and frequency offset. Also, the OFDM system can deal with the synchronization problem in time or frequency domain. As a result, it is considered to be more complicated than single carrier systems.

3.3.1 Packet Detection

Packet detection is to detect if a packet has arrived or not. It is the first function that the inner receiver has to perform. Other functions do not have to keep functional until a packet has arrived. There are two issues in packet detection. If a packet has actually arrived and not detected, we call it missing. If no packet has arrived but detected, we call it false alarm. Generally, a false alarm is a less severe than a missing packet since the missing always results in lost data.

There are many methods for packet detection. The repeated structure of the preamble enables the receiver to use a simple and efficient algorithm to detect the packet. Here, we use a common method called: "delay, correlated and normalized detection (DCND)"[12] . Define three variables c_n , p_n , and m_n as:

$$c_n = \sum_{k=0}^{L-1} r_{n+k} \cdot r_{n+k+D}^* \tag{3-10}$$

$$p_n = \sum_{k=0}^{L-1} (r_{n+k} \cdot r_{n+k}^* + r_{n+k+D} \cdot r_{n+k+D}^*) = \sum_{k=0}^{L-1} (|r_{n+k}|^2 + |r_{n+k+D}|^2) \tag{3-11}$$

$$m_n = \frac{4|c_n|^2}{(p_n)^2} \tag{3-12}$$

The delay D in above equations is equal to the period of the preamble. There are two windows called C and P windows and the window length is L. The C window

calculates a sequence of the crosscorrelation c_n between the received signal and its delayed version (delay and correlate). The P window calculates the received signal energy for the crosscorrelation window. The value of the P window is then used to normalize the decision statistic, so that it is not dependent on absolute received power level. When the decision variable m_n exceeds a predefined threshold, a packet is claimed to be detected. Figure 3-8 shows the operation of this algorithm.
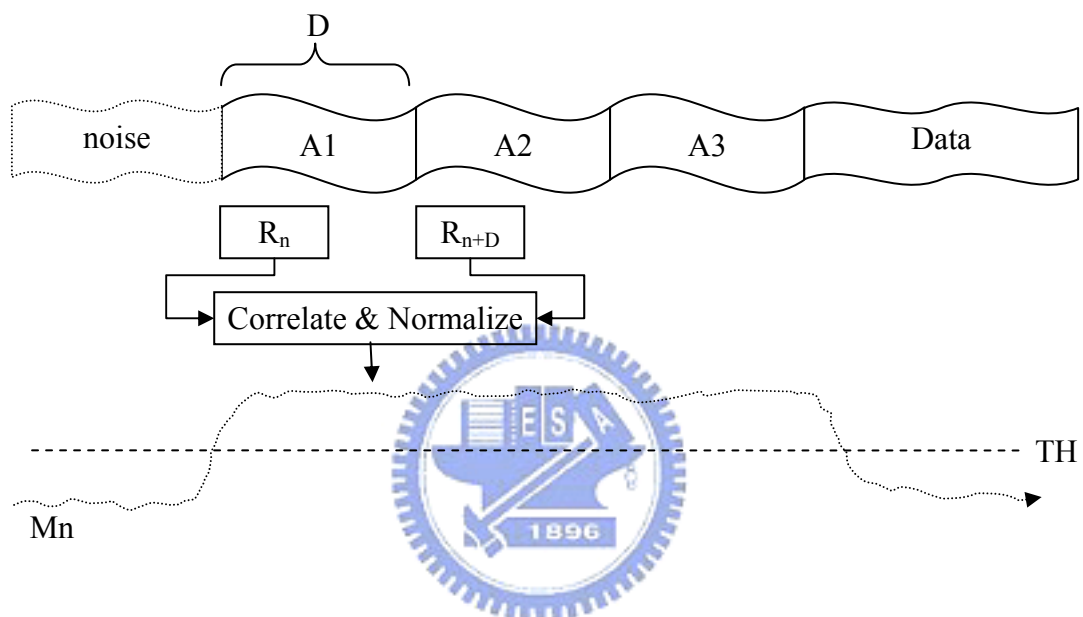
Figure 3-8 : Delay, Correlated and Normalized Detection

Figure 3-9 illustrates an example of the decision statistic for an IEEE 802.11n preamble. Note that the normalized decision variable is restricted between [0,1] and the start of the packet can be seen very clearly. When the received signal consists of noise only, c_n is a zero-mean random variable. This explains the low level of m_n before the start of the packet. Once a packet is received, c_n corresponds to a crosscorrelation of two identical preambles. Thus, m_n jumps up quickly to its maximum value.

Figure 3-9 : Response of the packet detection

As mentioned, the preamble of IEEE 802.16 contains only three approximately identical segments (since 2048 is not divisible by three). However, the packet detection algorithm used here can still do the job. We have actually interpolated the preamble to make it exactly periodical. However, the performance of packet detection is not significantly enhanced.
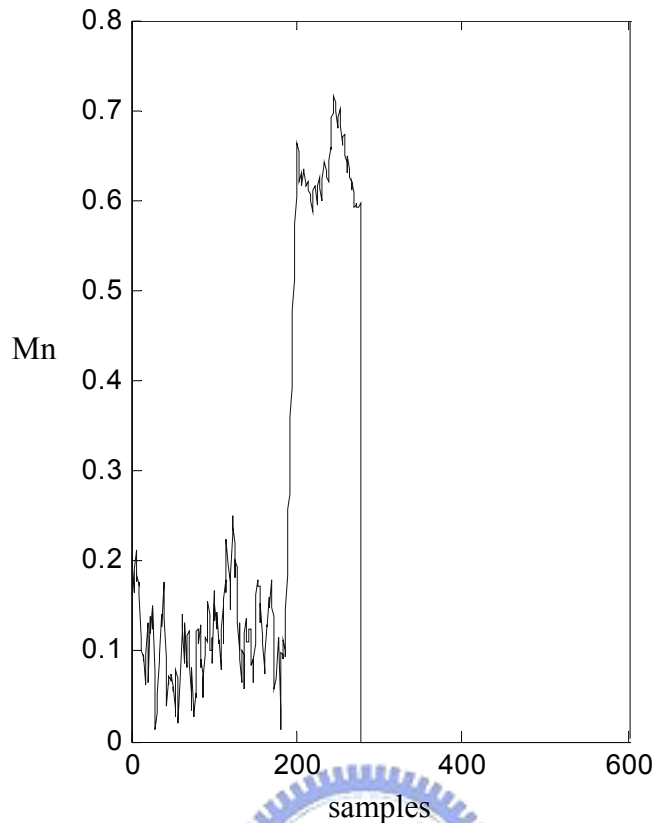
The approach outlined above is useful for high to normal SNR. Unfortunately, for low SNR, the decision statistic m_n may exceed the threshold even not packet is present. Thus, the probability of the false alarm will be increased. We can increase the threshold level; however, the probability of missing will be increased also. Here, we propose a modification to solve this problem. We add an extra window to accumulate the decision statistic. If most decision statistics (may be three forth) in the window are higher than the threshold, we then declare the detection of a packet. The rationale for

this approach is that if a packet actually arrives, the decision statistics m_n will remain high until the end of preamble. Simulations show that the modified approach can have more robust detection performance.

3.3.2 Frequency Synchronization

One of the main drawbacks of OFDM is its sensitivity to CFO. The effect has been outlined in Section 3.2.3. Many algorithms have been developed to estimate the CFO in OFDM systems [12] . One data-aided algorithm, exploring the periodic property of the preamble, allows the receiver to have the maximum likelihood estimate of the CFO. The method that operates on the time domain signal have been presented in several papers such as [11] . It requires at least two consecutive repeated OFDM symbols. As described in Section 3.1.2, the preamble of IEEE 802.16 has three approximately identical segments. This method is then applicable. We now develop the CFO estimator as follows.

Recall the received complex baseband signal (with CFO) as

$$
\begin{aligned}
r_n &= y_n \cdot e^{-j2\pi \cdot f_r \cdot nT_s} \\
&= s_n e^{j2\pi \cdot f_t \cdot nT_s} \cdot e^{-j2\pi \cdot f_r \cdot nT_s} \\
&= s_n e^{j2\pi \cdot (f_t - f_r) \cdot nT_s} \\
&= s_n e^{j2\pi \cdot f_\Delta \cdot nT_s}
\end{aligned}
\tag{3-13}
$$

Let D be the delay between the identical samples of the two repeated symbols and define an intermediate variable z as

$$
\begin{aligned}
z &= \sum_{n=0}^{L-1} r_n \cdot r_{n+D}^* \\
&= \sum_{n=0}^{L-1} s_n e^{j2\pi \cdot f_\Delta \cdot nT_s} \cdot \left(s_{n+D} e^{j2\pi \cdot f_\Delta \cdot (n+D)T_s} \right)^* \\
&= \sum_{n=0}^{L-1} s_n s_{n+D}^* \cdot e^{j2\pi \cdot f_\Delta \cdot nT_s} e^{-j2\pi \cdot f_\Delta \cdot (n+D)T_s} \\
&= e^{-j2\pi \cdot f_\Delta \cdot DT_s} \sum_{n=0}^{L-1} \left| s_n \right|^2
\end{aligned}
\tag{3-14}
$$

where L is the window length of the estimator. The CFO can then be estimated as

$$\hat{f}_\Delta = -\frac{1}{2\pi D T_s} \angle z \qquad (3\text{-}15)$$

Since the sampled preamble does not have exact three periods, we cannot find an integer D between identical samples. Note that the ideal delay D is $682\frac{1249}{1703}$. Thus, we can consider a linear interpolation to interpolate r_{n+D}. Then,

$$
\begin{aligned}
z &= \sum_{n=0}^{L-1} r_n \cdot r^*_{n+682\frac{1249}{1703}} \\
&= \sum_{n=0}^{L-1} r_n \cdot \left(\frac{454}{1703} r^*_{n+682} + \frac{1249}{1703} r^*_{n+683} \right) \\
&= \frac{454}{1703} \sum_{n=0}^{L-1} r_n \cdot r^*_{n+682} + \frac{1249}{1703} \sum_{n=0}^{L-1} r_n \cdot r^*_{n+683}
\end{aligned}
\qquad (3\text{-}16)
$$

This modification can increase the performance for CFO estimation.

A limitation of the CFO estimation method is its operation range, which defines how large the CFO can be estimated. The range is directly related to D. Note that $\angle z$ is equal to $-2\pi \cdot f_\Delta \cdot D T_s$, which is unambiguous only in the range $[-\pi, \pi]$. Thus if the absolute value of the CFO is lager than the limit shown below, the result will be incorrect.

$$|f_\Delta| \geq \frac{\pi}{2\pi D T_s} = \frac{1}{2 D T_s} \qquad (3\text{-}17)$$

The maximum CFO that can be estimated is then

$$f_{\Delta \max} = \frac{1}{2 D T_s} = \frac{BW}{2D} \qquad (3\text{-}18)$$

where the BW is the signal bandwidth for transmission. For example, if the bandwidth is 20 MHz and the ideal delay D is $682\frac{1249}{1703}$, then $f_{\Delta \max} = 14.65$ KHz.

The estimation range can be also explained in the frequency domain. If a symbol waveform repeats N times with a period with D samples, the signal in the frequency domain must repeat D times with the interval of N subcarriers i.e. of BW/D subcarriers.

45

Thus, the maximum CFO range can be estimated is $\pm \dfrac{BW}{2D}$, which is the same as that derived above. Figure 3-10 illustrates this relationship.
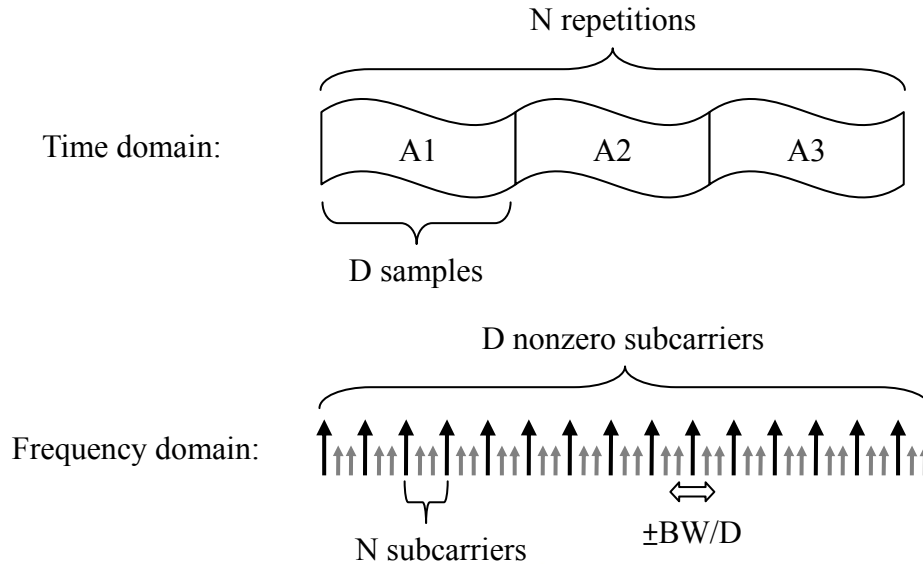

Figure 3-10 : Characteristic of the preamble of IEEE 802.16

3.3.3 Preamble Series Search

Since the preamble series transmitted depends on the segments and IDcell parameter, the receiver does not have any priori information regarding the preamble series it will receive. As a result, it has to find one from 114 possible preambles. From the found series, the receiver can have the information of the used segment and the IDcell. This search procedure can be divided into two steps. The first step is to determine which segment the received preamble belongs to, and the second one is to determine which preamble completely matches the received preamble.

The preamble data for each segment uses one third of subcarriers. Subcarriers for segment 0 and for segment 1 (segment 2) are shifted by one subcarrier spacing. We can use this property to determine the segment used. This is shown in Figure 3-1. From the figure, we can see that the segment 0 modulates the preamble data within the carrier-set 0 (including the DC subcarrier). Thus, when there is no CFO, the CFO

estimator will give the zero value. The segment 1 modulates the preamble data within the carrier-set 1 right-shifted from the carrier-set 0. Thus, when there is no CFO, the CFO estimator will give the amount of one subcarrier spacing δ. On the contrary, the carrier-set 2 for segment 2 is obtained from the left-shifted carrier-set 0. So, the CFO estimator will give $-\delta$. We then conclude that if the range of CFO is smaller than 0.5δ, the receiver can determine the segment with the CFO estimator. When the CFO estimator gives the offset larger than 0.5δ, the segment one is determined. When the estimator gives the offset smaller than -0.5δ, the segment two in determined.

After determining which segment the received preamble belongs to, we can go to the second step to find which preamble is received. Since the preamble series is modulated by a pseudo random series, a simple correlator can be used to match the received preamble waveform. Note that there are 38 preamble series for each segment to be matched. However, the computational complexity will be high for this approach. To solve the problem, we can use a frequency domain approach. Note that the correlation in the time domain is equivalent to the multiplication in the frequency domain. To do that, the received preamble must first be transformed to the frequency domain (with DFT), multiplied by the conjugate of the preamble series, and then transformed back to the time domain (with IDFT). This process is shown in Figure 3-11. Finally, the preamble with the maximum absolute peak value is chosen as the output. Mathematically, it can be expressed as follow:

$$\hat{l} = \arg\max_{l} \left| IDFT\left\{ \sum_{k=0}^{K} R[k] \cdot P_l[k] \right\} \right|^2 \qquad l = 0,\cdots,37 \qquad (3\text{-}19)$$

In (3-19), the subcarrier index k ranges from 0 to K (DFT size), $R[k]$ is the received preamble (in the frequency domain), the $P_l[k]$ is the known preamble series (one of

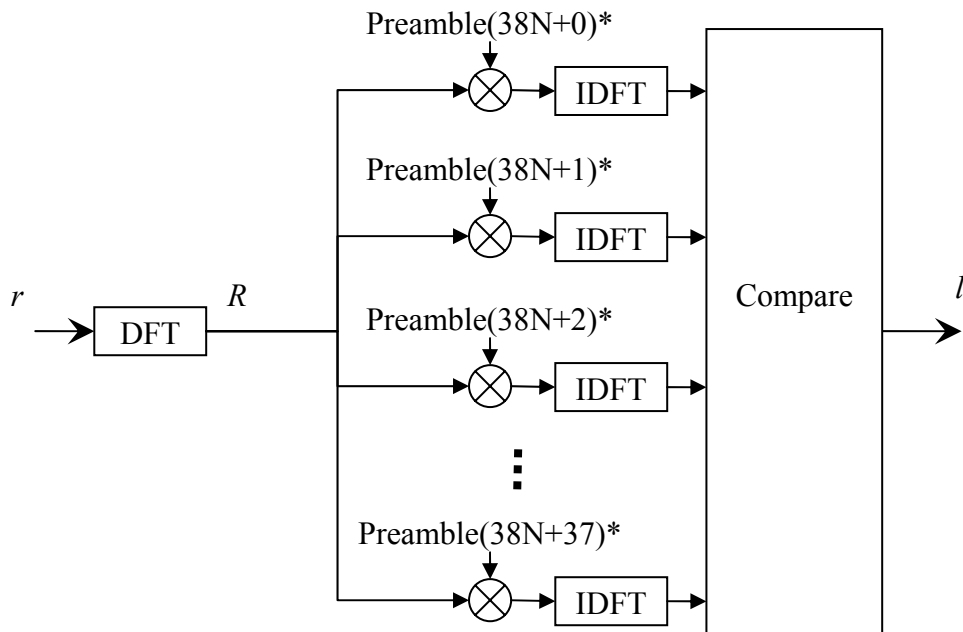38 preambles), and *l* is the preamble number index.

Figure 3-11 : Multiplication approach of the preamble series search

Figure 3-12 shows an example of this operation; it is the result of matching preamble series in segment 0 (after IDFT).
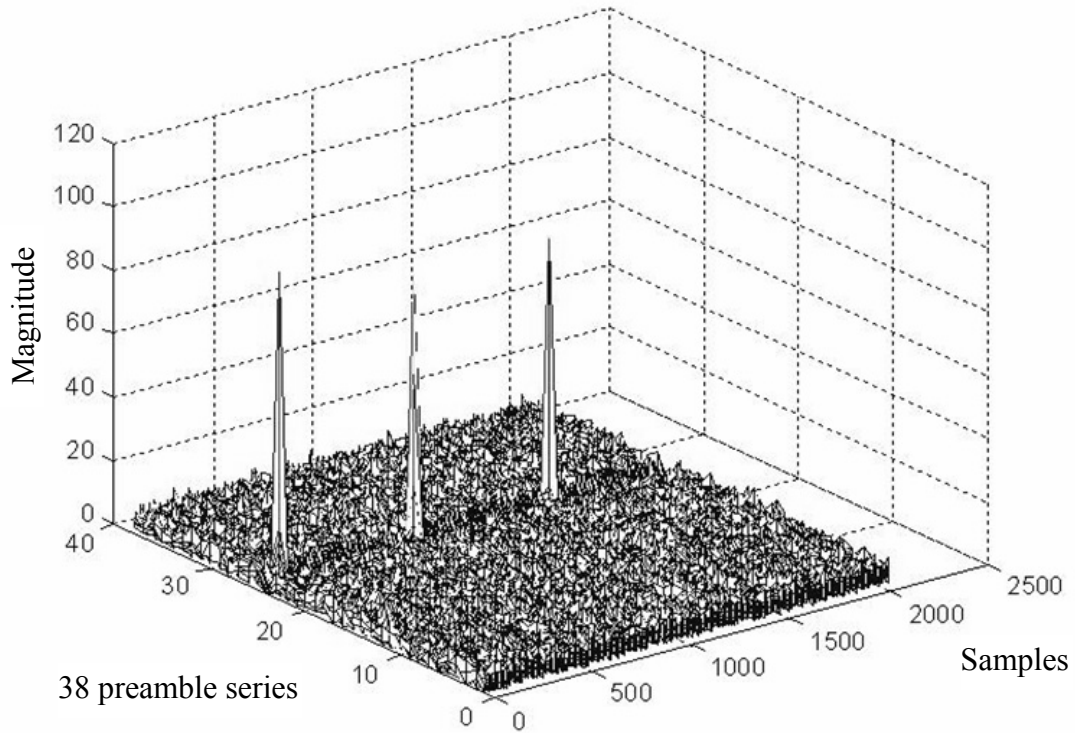

Figure 3-12 : Result of the multiplication approach for full size (2048) IDFT

This approach needs to perform full DFT/IDFT operations, 2048 points for IEEE 802.16-2004. However, note that the preamble series only occupies 568 subcarriers; values for other subcarriers are all zeros. Here, we give a modified algorithm that can save computations. After the received preamble is transformed to the frequency domain with a 2048-point DFT, the 568 subcarriers the received preamble occupied are multiplied by a specific preamble series. The result is then transformed back to the time domain with a 568-point IDFT. The computational complexity of the multiplication and IDFT operations becomes smaller. Figure 3-13 show an example of the final result.
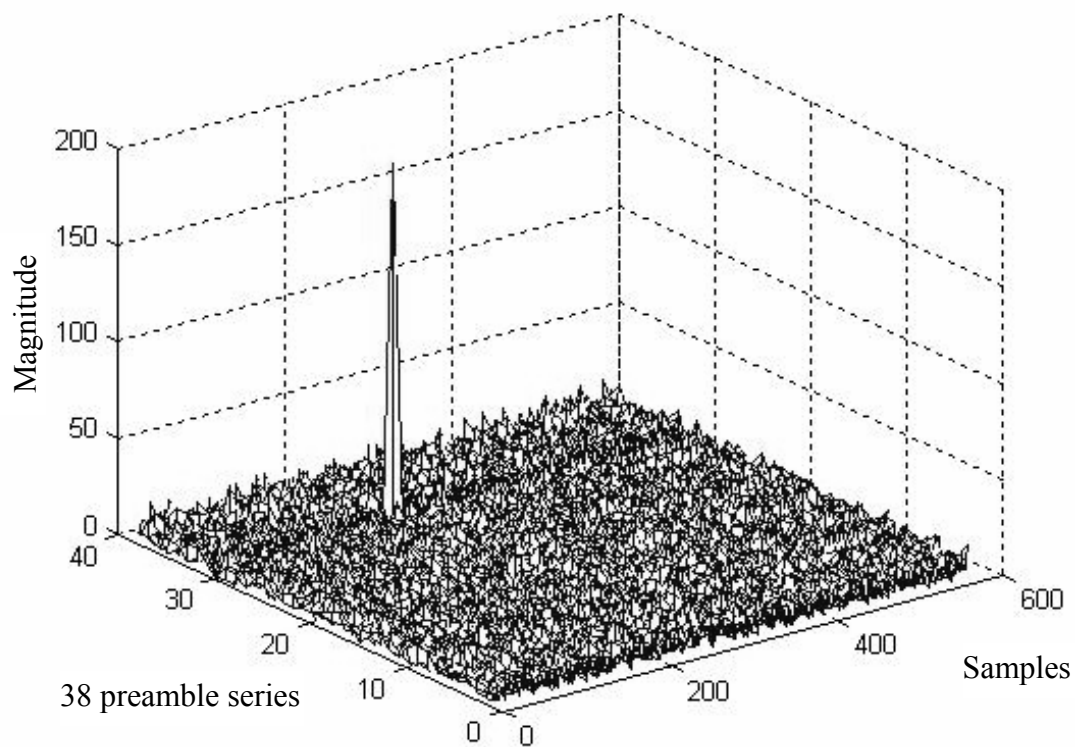
Figure 3-13 : Result of the modified approach for small size (568) IDFT

3.3.4 Symbol Timing Offset Estimation

The objective of symbol timing offset (STO) estimation is to locate the edge of

an OFDM symbol. The result is used to define the DFT window, a set of samples for

the DFT operation. Since the preamble is available to the receiver, it enables the

receiver to use the simple correlation-based STO algorithm. After the packet is

detected, the start of the packet is roughly located. The STO refines the precision to

the sample-level. Thus, the packet detection can be regarded as a coarse symbol

timing synchronization, and the symbol timing correction as a fine symbol timing

synchronization.

As mentioned, we use the correlation-based algorithm and it can be expressed as

follows.

$$\hat{t}_s = \arg\max_n \left| \sum_{m=0}^{L-1} r_n[m] \cdot p[m] \right|^2 \qquad (3\text{-}20)$$

where $r_n[m]$ is the received preamble and $p[m]$ is the known preamble. The value of n that corresponds to maximum absolute value of the correlation is the STO estimate t_s and the L is the length of the correlated window. Figure 3-14 shows an example of the output of correlator that uses the last 16 samples of the short preamble and the 32 samples of the long preamble in IEEE 802.11n system. The peak value can be found close to the sample index 20 that is the idea symbol boundary. The figure shows two curves corresponding to the results of two different channels.
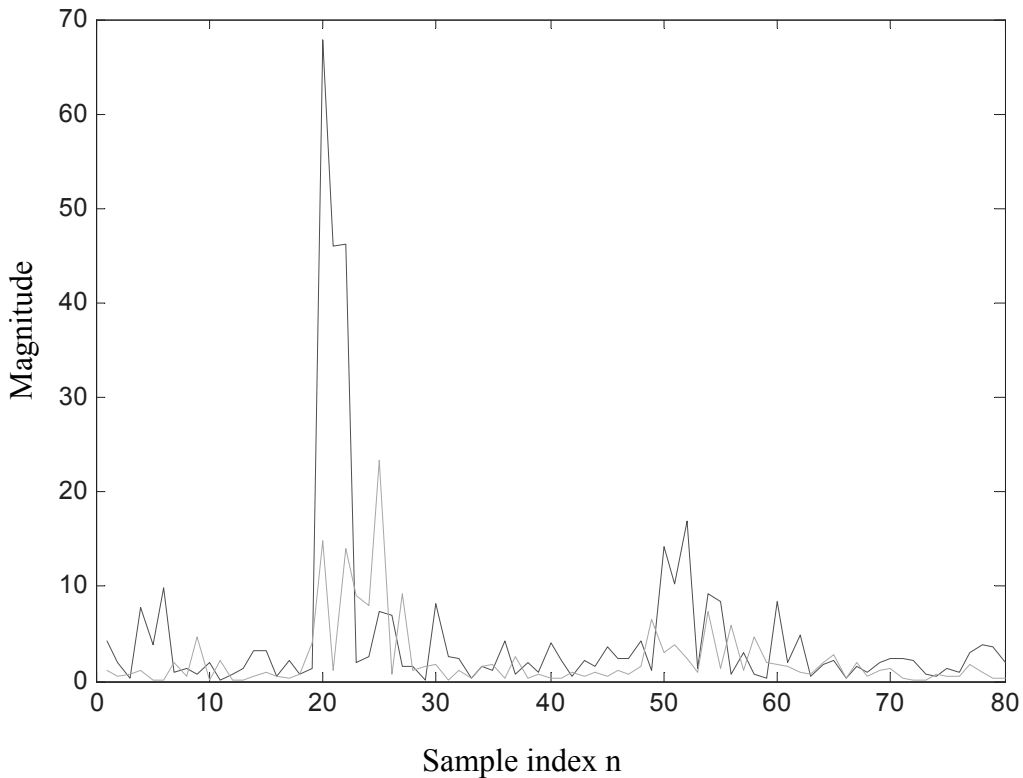

Figure 3-14 : Response of the symbol timing crosscorrelator

Note that the correlation operation for the STO estimation has been completed in the preamble series search. No extra computations are required. After determining the preamble series, the receiver can also determine the sample index n corresponding to the maximum value. Thus, we can combine these two functions and the result is
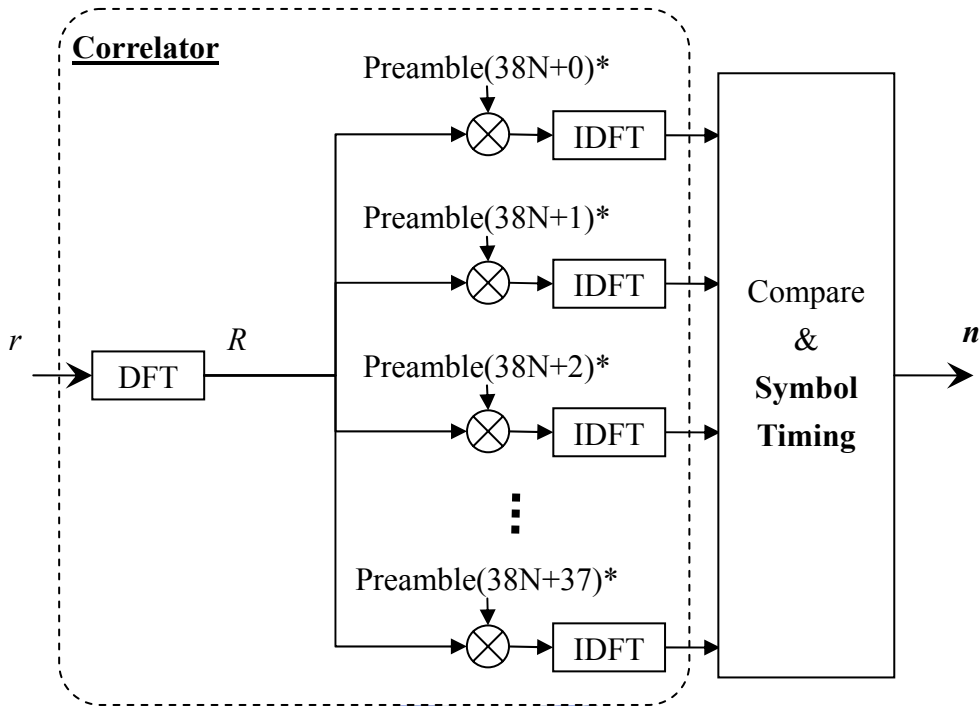
shown in Figure 3-15.

Figure 3-15 : Structure of the combination approach

If we use the modified preamble series search method, we only have the result of

568-point IDFTs. Thus, the output of the correlator only has 568 instead of 2048

points. However, the STO estimate should have the precision down to the sample

level i.e. 2048 points. So the sample index n that corresponds to the maximum value

has to be re-evaluated.

From Figure 3-1, we can see that there are 1704 used subcarriers for preambles

(excluding the guard band). The rest of subcarriers can be seen as zero padding. Thus,

the sampling period for the time domain signal will become larger if the 1704-point

IDFT is used. The actual preamble is modulated with one third of 1704 subcarriers i.e.

568 subcarriers; it can be seen as the result of downsampling (downsampling factor is

three) the original 1704 subcarriers. The down sampling operation causes the time

domain signal to be overlapped and added. Thus, if we use 568-point IDFT for

preamble search, we can obtain the corresponding time domain signal by dividing the 1704-point IDFT signal into three parts, overlapping these three parts, and adding them together. Figure 3-16 depicts these two parts of the transformation.
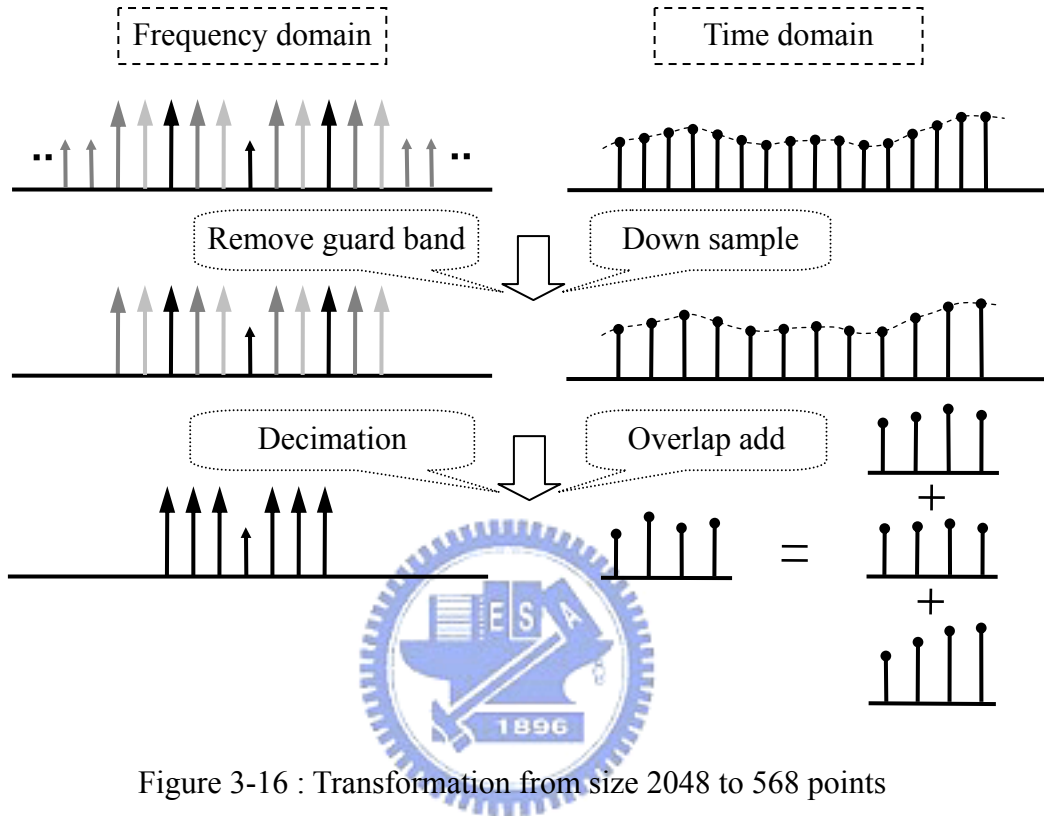

Figure 3-16 : Transformation from size 2048 to 568 points

With the original 2048-point IDFT size approach, the resultant signal of the correlator (IDFT) will give three peaks if the preamble has been matched. Theoretically, the three peaks have a periodic property and any one of peak positions can be used to find the STO. In other words, we can divide the time domain signal into three parts and overlap them together without affecting the STO estimation. For the 1704-point IDFT, the property still holds. The only difference lies in the sampling period (in the time domain) in this case is larger and the peak position has to be adjusted. The following equation gives the formula for the adjustment.

$$\hat{t}'_s = \frac{2048}{1704}\hat{t}_s = \frac{2048}{1704}\arg\max_n \left| \sum_{m=0}^{L-1} r_n[m] \cdot p[m] \right|^2 \qquad L = 568 \qquad (3\text{-}21)$$

3.3.5 Channel Estimation

The objection of channel estimation is to estimate the frequency response of the channel. With the information, the original transmitted signal can be recovered. Here, we consider data-aided channel estimation. That means transmitted symbols for subcarriers have to be known. In 802.16, we have two places where known symbols can be found. The first one is the preamble, and the second one is the pilot signal. Since the number of known subcarriers in the preamble is large (568), its estimation accuracy is higher. However, when the channel is time-variant, the estimate may not be useful for later data symbols. Nevertheless, it can be used to recover the data in FCH and DL-MAP. Pilots are inserted in data symbols; its number is limited. The channel estimate is then less accurate, but it can track the channel variation. Since the preamble and the pilots are not placed on all subcarriers, interpolation is then needed to obtain the channel responses of other subcarriers.

The received for the preamble or pilots can be expressed as

$$R_l[k] = H_l[k] \cdot X_l[k] + W_l[k] \tag{3-22}$$

where $H_l[k]$ is channel frequency response, $X_l[k]$ is transmitted known data, $W_l[k]$ is AWGN, all for the k th subcarrier and the lth symbol. The channel estimation can be calculated as

$$
\begin{aligned}
\hat{H}_l &= R_l \cdot X_l^* \big/ |X_l|^2 \\
&= (H_l \cdot X_l + W_l) \cdot X_l^* \big/ |X_l|^2 \\
&= (H_l \cdot |X_l|^2 + W_l \cdot X_l^*) \big/ |X_l|^2 \\
&= H_l + W_l \cdot \frac{X_l^*}{|X_l|^2}
\end{aligned} \tag{3-23}
$$

As mentioned, interpolation is required. For low to moderate mobile speed, the

special interpolation can have satisfactory results. However, for high speed mobile

environment, straightforward linear interpolation cannot met the requirement. A

simple and effective interpolation scheme has been developed in [17] . In this thesis,

we will use the method to conduct channel estimation. For details, please see [17] .

Chapter 4: Simulation Results

In this chapter, we conduct simulations to evaluate the performance of the designed transceiver for OFDMA PHY of IEEE 802.16-2004. The transmitter and receiver use 2048-point FFT and IFFT. We build the physical frames of three segments and choose four frames of two segments for the four receivers, as shown in Figure 4-1. Then, we have four subscriber stations (SS) to receive the signal of one base station (BS). Two of four SSs are in segment 1 (from 0) and other two SSs are in segment 2.
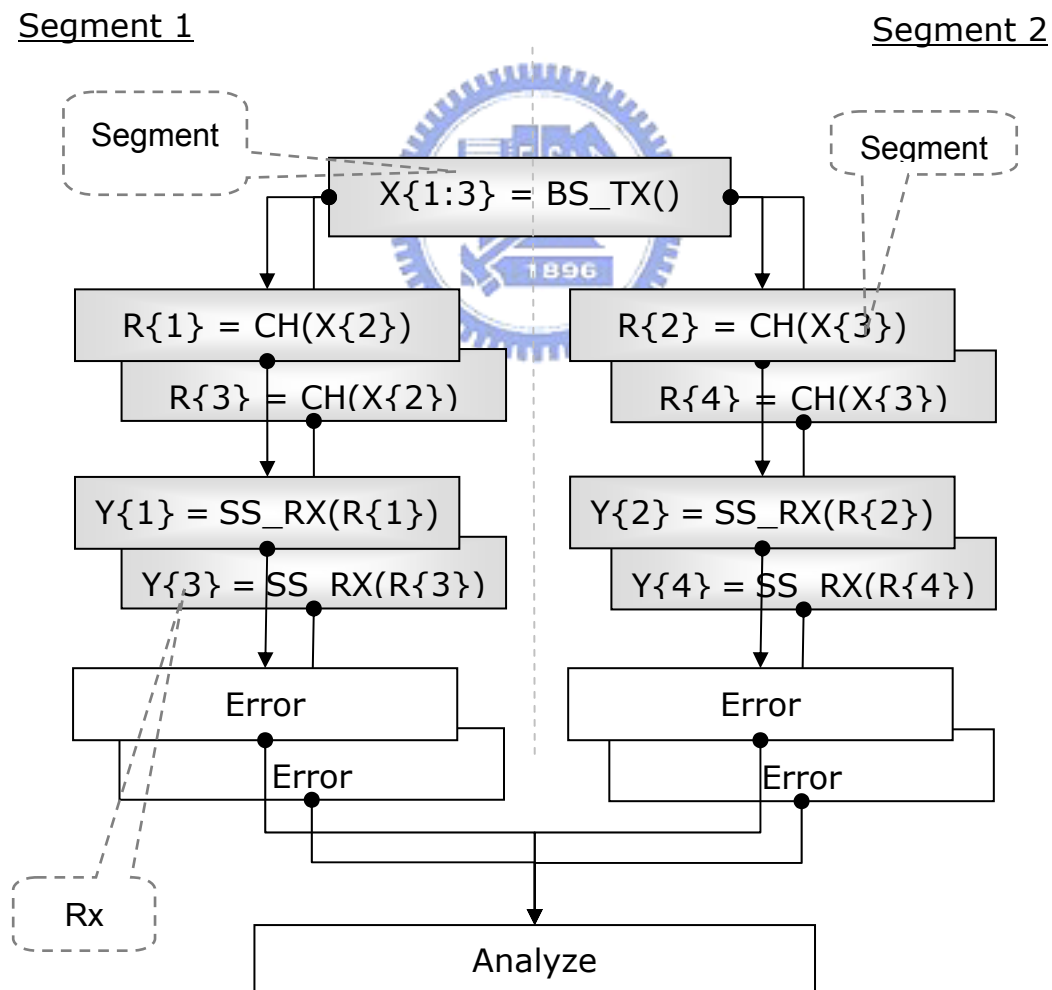

Figure 4-1 : Structure of simulation

We will evaluate the BER (bit error rate) in various channel impairment settings such as: simple AWGN, multi-path fading channel, frequency offset, and timing offset. In every circumstance, the ideal results (the channel effects are known) will be shown first, the results corresponding to channel impairment (the channel effects are unknown) will be shown next, and the compensated results (the channel effects are estimated) will be shown finally.

4.1 Introduction

Figure 4-2 and Figure 4-3 illustrate the frame structure of segment one and segment two. There are four bursts in each segment; the first burst is a broadcast burst and other three bursts are the unicast bursts. In the simulation, the first one of four SSs receives the broadcast burst and burst 1 in segment one, the second one receives the broadcast burst and burst 2 in segment one, the third one receives the broadcast burst and burst 1 in segment two, and the last one receives the broadcast and burst 2 in segment two.

In segment one, the length of the broadcast burst (Bb) is 1000 bytes, length of the 1st burst is 720 bytes, and length of the 2nd burst is 930 bytes.
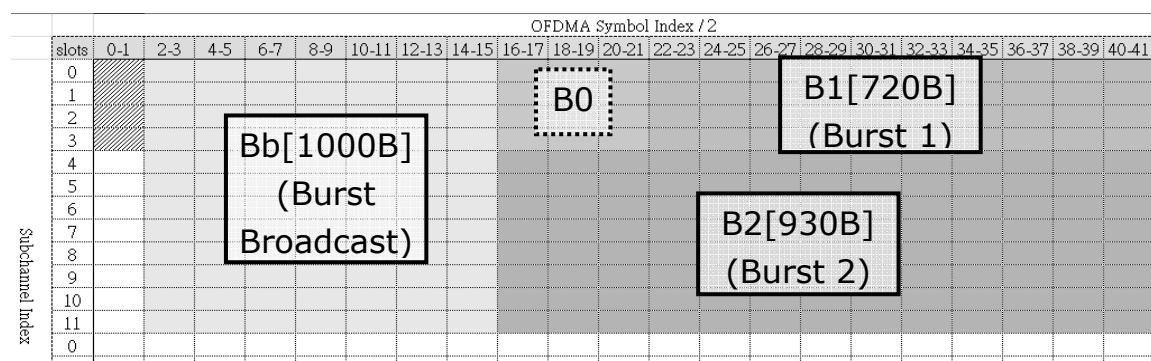

Figure 4-2 : Frame structure of the segment one

In segment two, the length of the broadcast burst (Bb) is 360 bytes, length of the

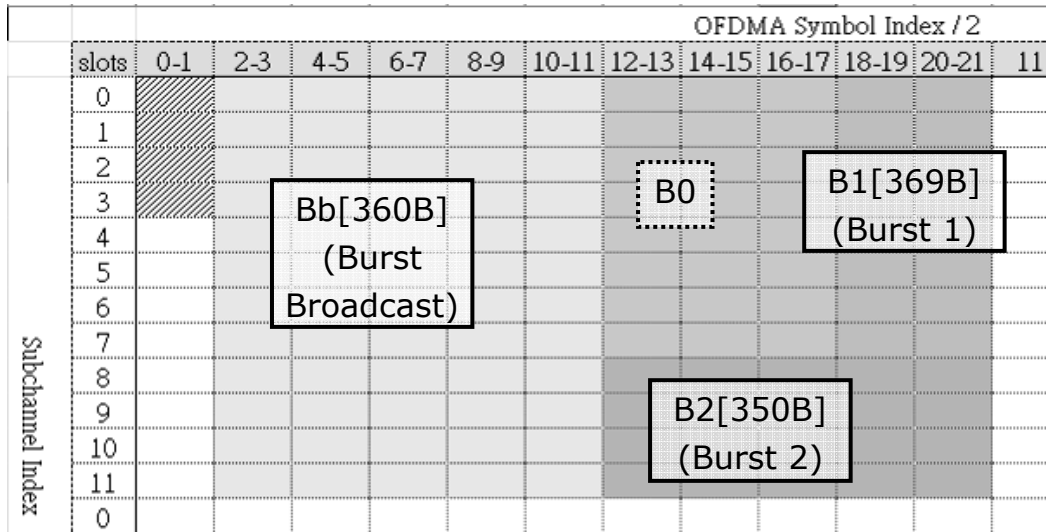1st burst is 369 bytes, and length of the 2nd burst is 350 bytes.

Figure 4-3 : Frame structure of the segment two

All broadcast bursts in all segments use 16QAM and 1/2 coding rate, the 1st burst (B1) in segment one (S1) uses 64QAM and 1/2 coding rate, the 2nd burst (B2) in S1 uses QPSK and 3/4 coding rate, the B1 in S2 uses 64QAM and 2/3 coding rate, and the B2 in S2 uses 16QAM and 3/4 coding rate, as shown in Table 4-1.

Segment	Burst	Modulation and Coding
S1	Bb	16QAM 1/2
S1	B1	64QAM 1/2
S1	Bb	16QAM 1/2
S1	B2	QPSK 3/4
S2	Bb	16QAM 1/2
S2	B1	64QAM 2/3
S2	Bb	16QAM 1/2
S2	B2	16QAM 3/4

Table 4-1 : Coding rate and modulation type of the bursts

4.2 AWGN

In this set of simulations, the channel is AWGN and SNR used ranges from 2 dB to 10 dB. Figure 4-4 shows the bit error rate (BER) performance.
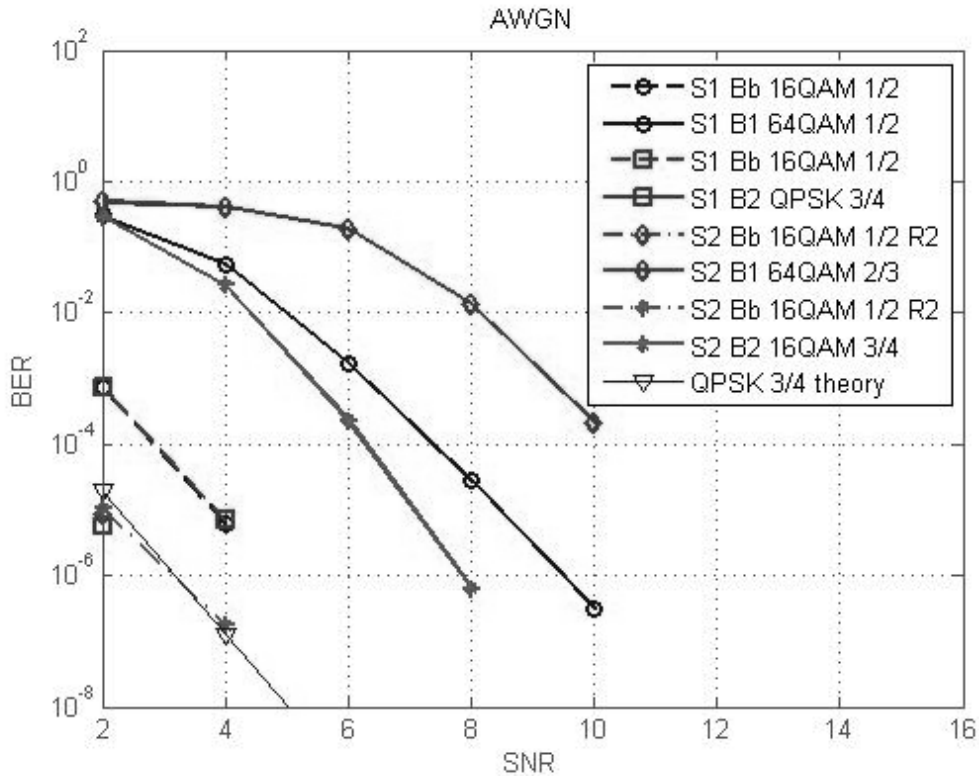
Figure 4-4 : BER performance with AWGN channel

We can see that the results for 16QAM and coding rate of 1/2 are the best and the result of 64QAM and coding rate of 2/3 isX the worst. However, all broadcast bursts of the segment one and segment two are the same (16QAM and coding rate of 1/2), but the performance for segment two is better than that for segment one. The reason may be that the bursts of the segment two are smaller than the burst of the segment one.

4.3 Multipath Channel

In the simulation, we use the urban macro-cell environment and vehicle's speed is set as 100 Km/hr. This channel is a NLOS multipath slow fading channel. There are 6 taps (paths) in the channel impulse response and the channel length is under 150 samples.

Figure 4-5 and Figure 4-6 shows the performance comparison for the cases that the
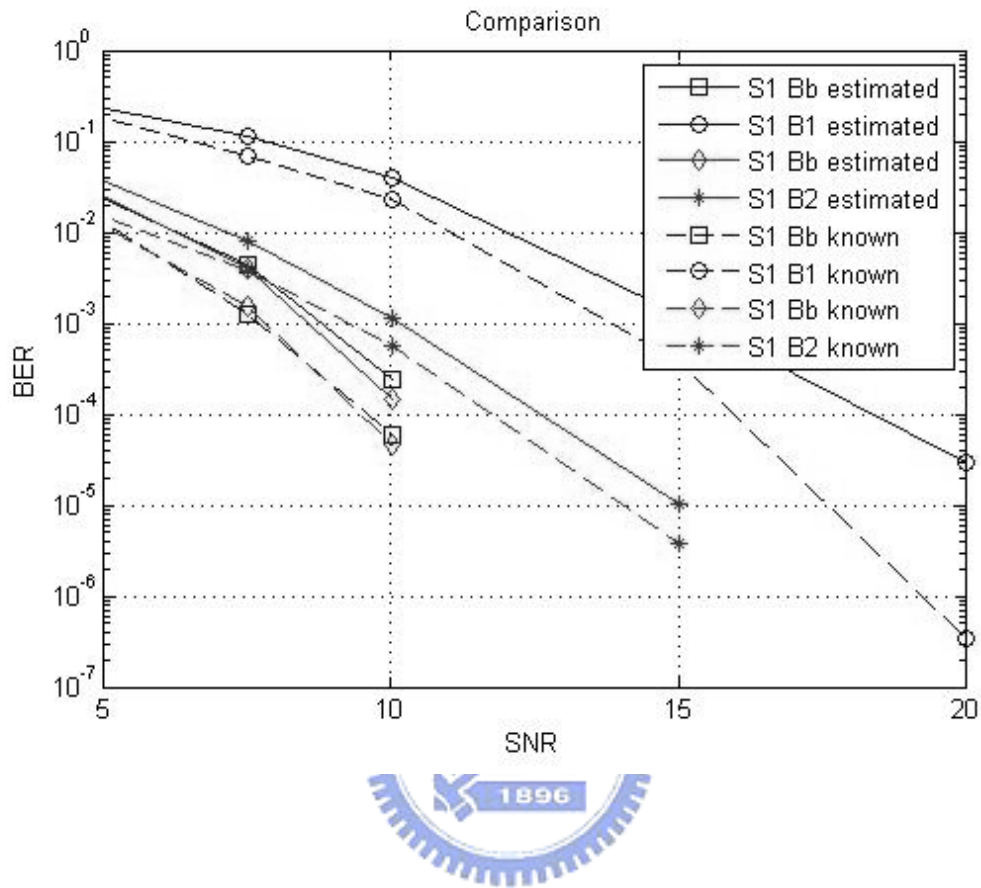
channel is known and estimated.

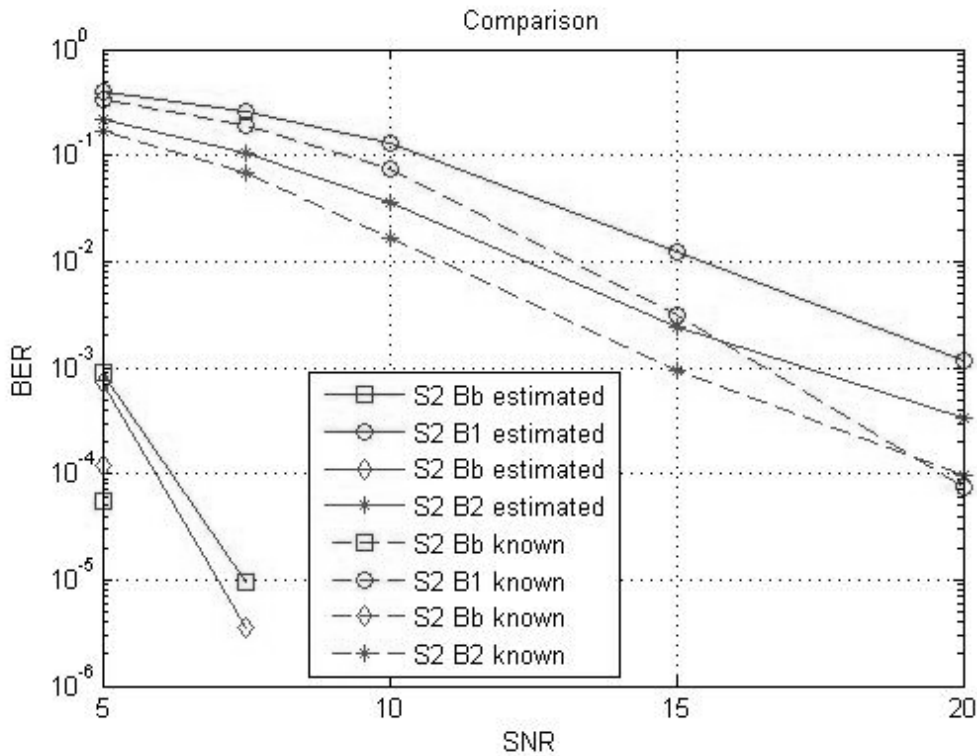Figure 4-5 : Comparison between the known and estimated channel for segment one

Figure 4-6 : Comparison between the known and estimated channel for segment two

It is obvious that the results with channel estimation are worse.

4.4 Timing Offset

This scenario is designed to evaluate the performance of packet detection and symbol timing offset estimation. The multipath channel information is estimated. The 2048 noise samples are added in front of each frame to simulate the unknown timing for the receiver.

Figure 4-7 and Figure 4-8 shows the comparison for the case that the timing offset is zero (packet detection and symbol timing perfectly detect timing), the timing offset is estimated, and the offset is unknown (packet detection estimated timing but symbol timing fixes timing equal to the length of CP).
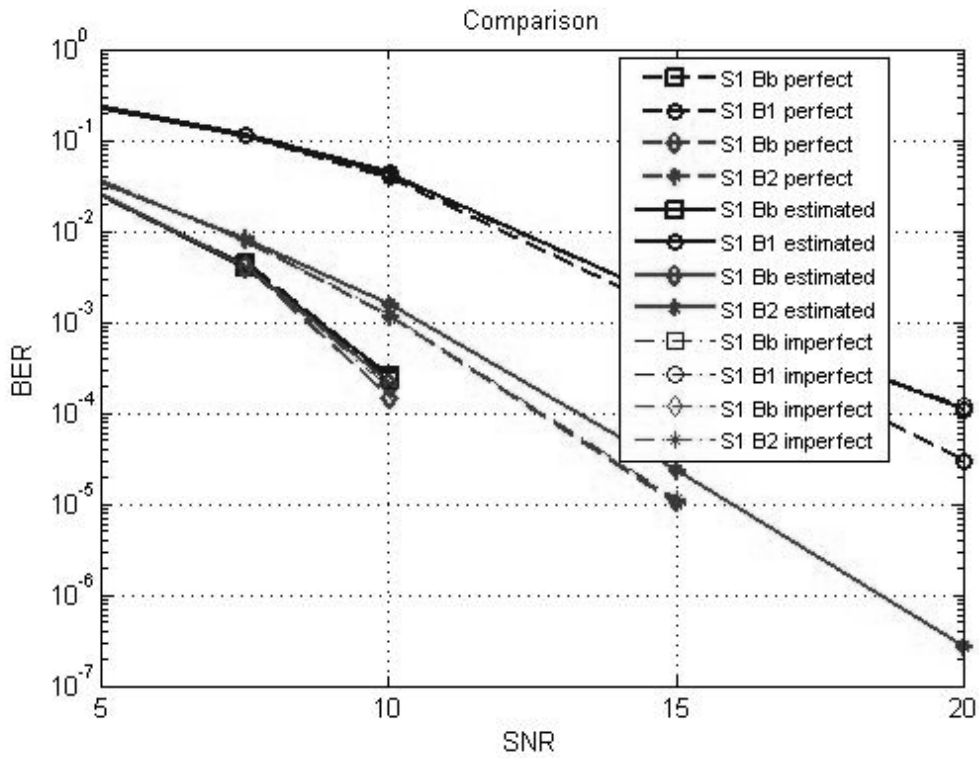
61

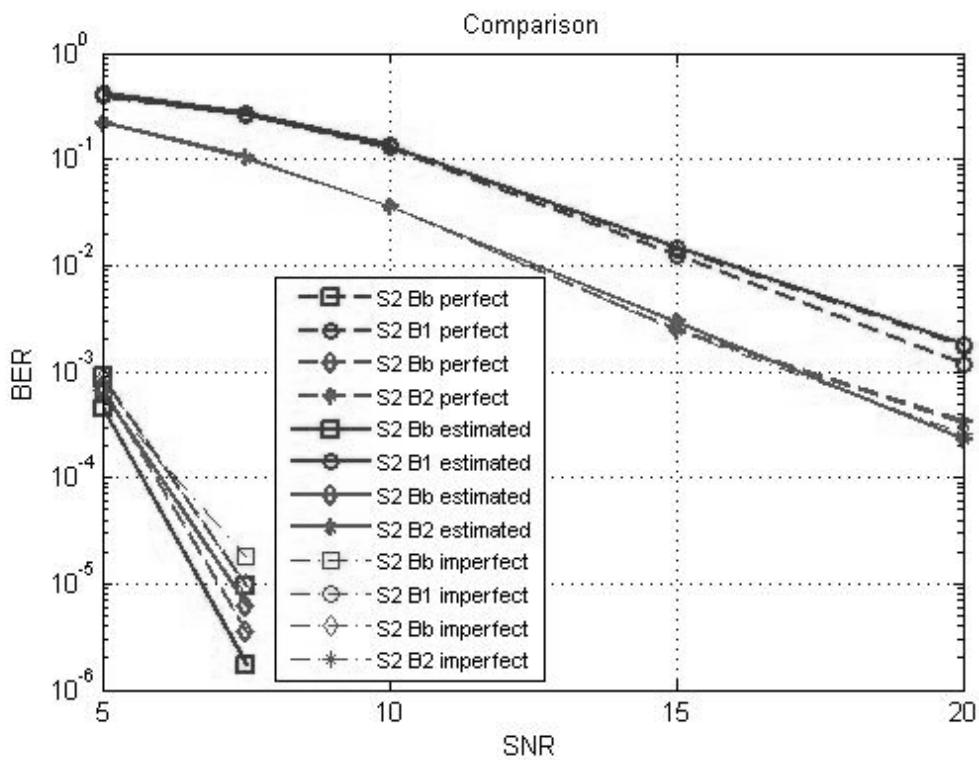Figure 4-7 : Comparison between the known and detected offset for segment one

Figure 4-8 : Comparison between the known and detected offset for segment two

There is no significant difference of these conditions because the length of CP (256sample) is quite larger than the length of multipath channel. It leads to that the timing offset is not large enough to cause the obvious ISI.

4.5 Carrier Frequency Offset

This scenario is designed to evaluate the performance of frequency synchronization. Similar timing simulation, the channel information is estimated but timing offset is perfectly detected. The CFO is equal to 0.26ppm of the carrier frequency 2GHz.

Figure 4-9 and Figure 4-10 shows the comparison for the case that CFO is known, is estimated and is unknown at all.
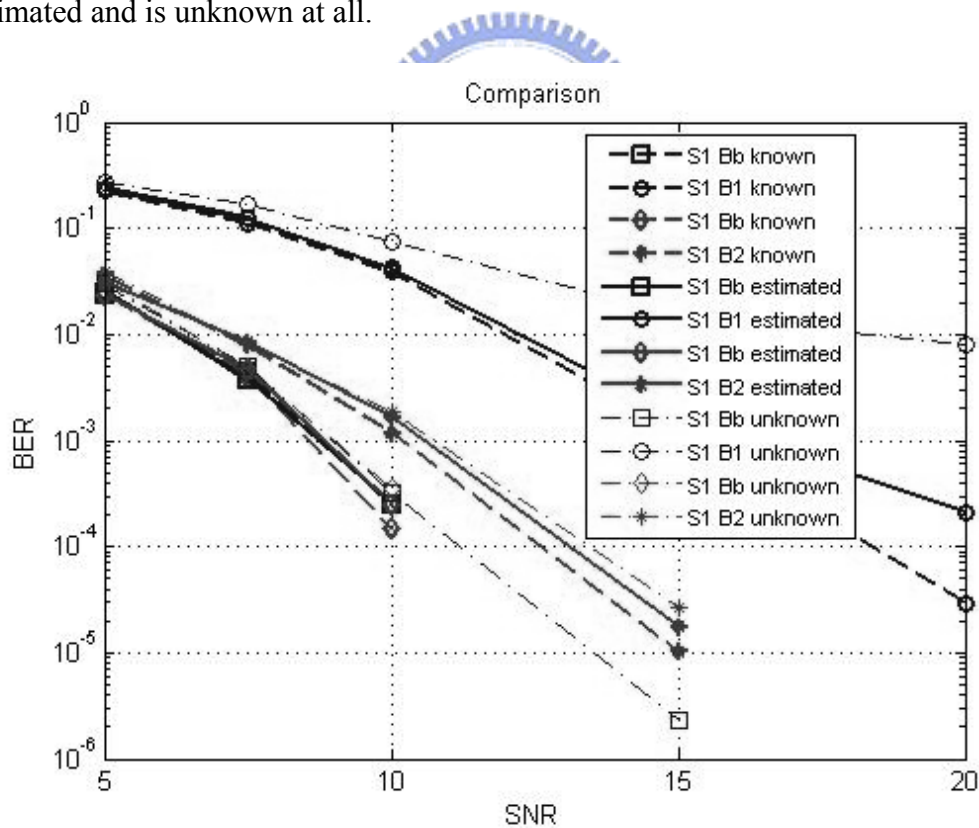

Figure 4-9 : Comparison between the known and estimated offset for segment one
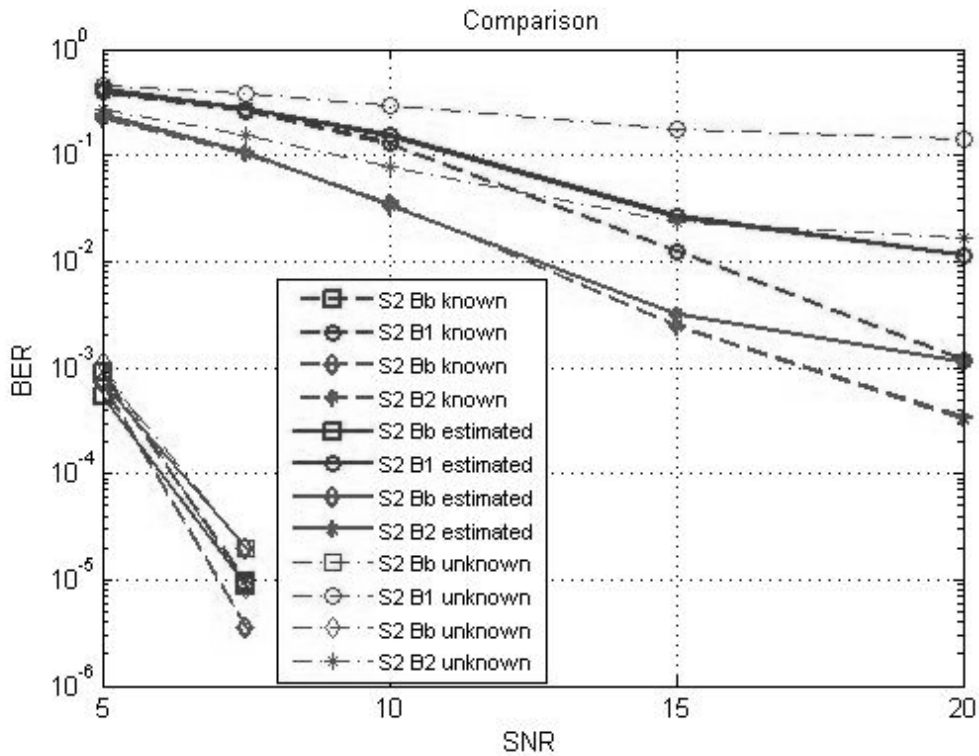
Figure 4-10 : Comparison between the known and estimated offset for segment two

The performance would be significantly degraded under the CFO effect if frequency synchronization is not operated since the CFO cause not only a phase shift but also an error of preamble searching.

4.6 All Effects

All above channel effects are combined for testing all inner receiver function.

Figure 4-11 and Figure 4-12 shows the comparison for the case that all channel effects are known, are estimated, and are even unknown.
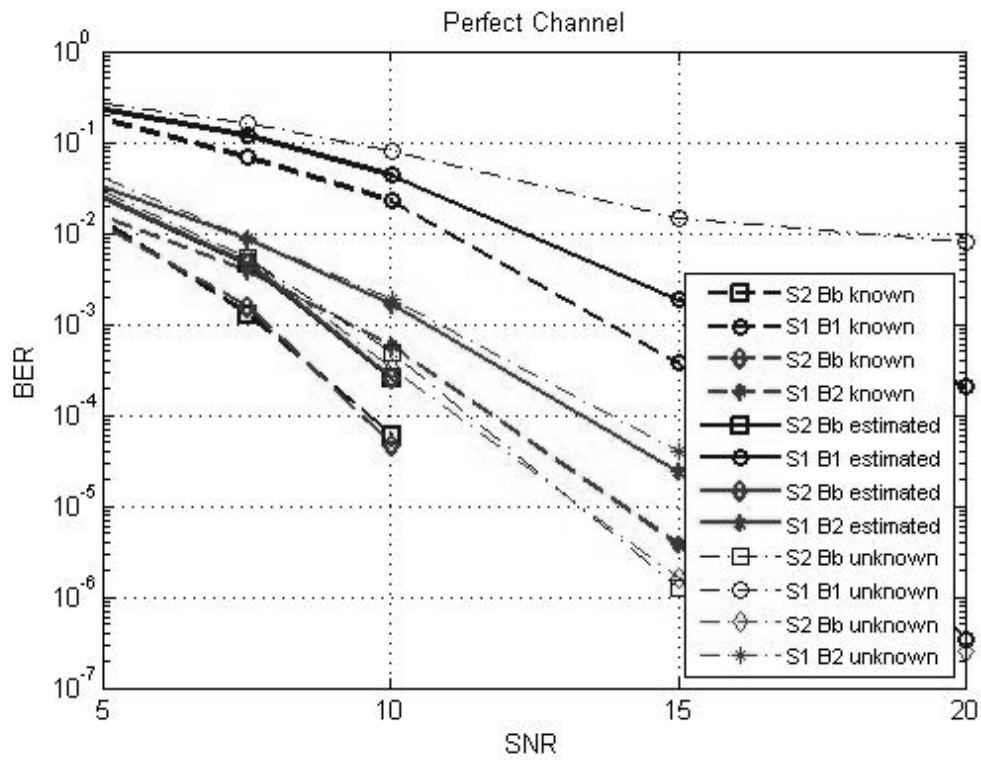
Figure 4-11 : Comparison between the known and estimated channel information for
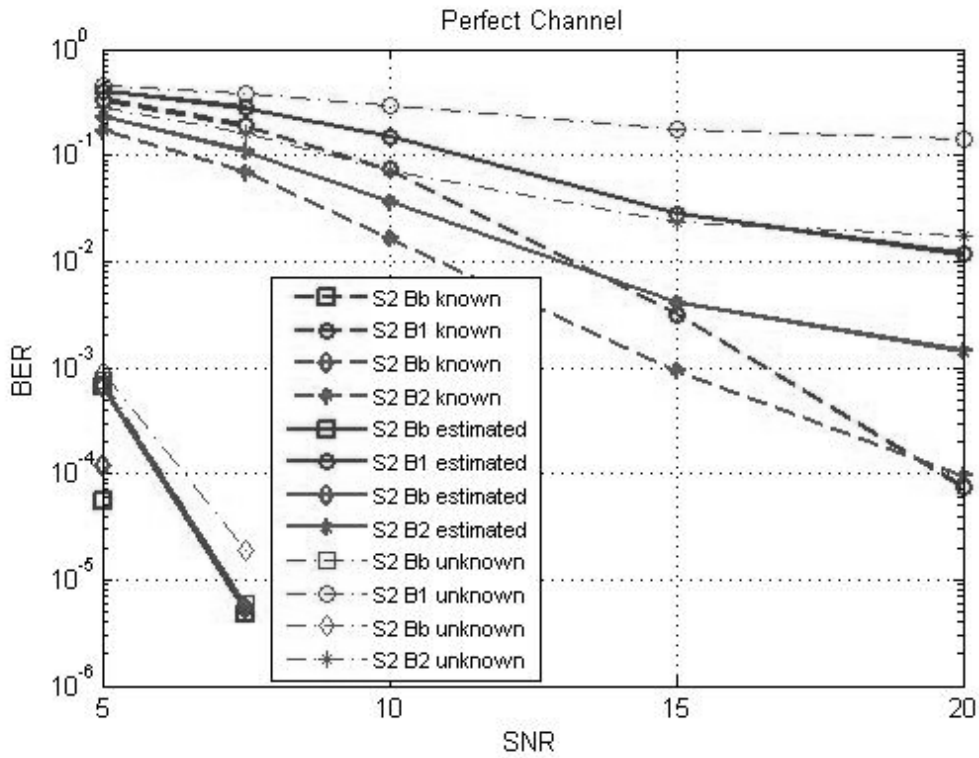
segment one

Figure 4-12 : Comparison between the known and estimated channel information for segment two

All above effects considered together lead to a great performance decay. However, the functions of the inner receiver could resist some effects to increase the performance.

Chapter 5: Conclusions

A downlink baseband system for IEEE 802.16 OFDMA mode has been studied in this thesis. As we can see, the IEEE 802.16 PHY has many standards; framing and signaling are complicated. Also, there are many options for real-world implementation. In this these, we mainly focus on the OFDMA system, which can improves the bandwidth efficiency in mobile and multiple access environments.

The transmitter of an IEEE 802.16 OFDMA system contains two main processing modules. One is the channel coding, including concatenation, data randomization, convolutional encoder, repetition encoder, and modulation. The other is the subcarrier allocation, including data mapping, permutation, renumbering, subcarrier randomization, and pilot insertion. After performing IDFT and adding CP, the transmitter sends the signal through the wireless channel. Channel effects such as the multipath fading, timing offset, and frequency offset, etc. have also been considered. These effects will distort the transmit signal and make the data recovery challenging in the receiver.

The receiver can be further divided into an inner and an outer receiver. The outer receiver reverses the operations performed in the transmitter. The function of the inner receiver is to cope with the channel effects; it performs signal synchronization, including packet detection, frequency synchronization, preamble series search, symbol timing offset estimation, and channel estimation.

The whole baseband system has been successfully implemented and its performance has been evaluated. From the simulation results, we can find that the channel estimation has significantly influence on the system performance, particularly

when the mobile speed of SS is high. The proposed channel estimate is simple and effective. It can have satisfactory performance for low and moderate mobile speed. For higher mobile speed, more sophisticated method has to be developed. Another problem deserve further study is the series search. When the SNR is low, it will become difficult to have a reliable result.

In this thesis, we study the basic functions of the IEEE 802.16 OFDMA downlink system. For subcarrier allocation, we only study PUSC. Other methods, such as FUSC or AMC, are not discussed in the thesis. Moreover, there are four FFT sizes in the IEEE 802.16e. We only study the size of 2048. The uplink system is not studied either. These can serve as topics for further study.

Reference

[1] Syed (Aon) Mujataba, IEEE802.11-04-0889, "TGn Sync Proposal Technical Specification," July 2005

[2] IEEE 802.16-2004, "Part 16: Air Interface for Fixed Broadband Wireless Access Systems," IEEE Std 802.16-2004

[3] IEEE 802.16e, "Part 16: Air Interface for Fixed and Mobile Broadband Wireless Access Systems," IEEE Std 802.16e-2005

[4] IEEE 802.11a, "Wireless LAN Medium Access Control (MAC) and Physical Layer (PHY) Specifications," IEEE Std 802.11a-1999

[5] R. W. Chang, "Synthesis of Band-Limited Orthogonal Signals for Multichannel Data Transmission," Bell Syst. Tech. J., Vol. 45, pp. 1,775-1,796, Dec. 1966.

[6] Weinstein, S, Ebert, P. "Data Transmission by Frequency-Division Multiplexing Using the Discrete Fourier Transform," Communications, IEEE Transactions on [legacy, pre - 1988] Vol. 19,　Issue 5,　Oct 1971 Page(s):628 - 634

[7] A. Peled and A. Ruiz, "Frequency Domain Data Transmission Using Reduced Computational Complexity Algorithms," IEEE International Conference on ICASSP '80, Vol. 5, April 1980, pp 964-967

[8] M. Speth, D. Daecke, H. Meyr, "Minimum Overhead Burst Synchronization for OFDM," IEEE International Conference on Communications, Vol. 3., 1996, pp 1301-1306

[9] M. Speth, S. Fechtel, G. Fock, and H. Meyr, "Optimum Receiver Design for Wireless Broad-Band Systems Using OFDM-Part I," IEEE Transactions on Communications, Vol. 47, No. 11, November 1999

[10] M. Speth, S. Fechtel, G. Fock, and H. Meyr, "Optimum Receiver Design for Wireless Broad-Band Systems Using OFDM-Part II," IEEE Transactions on

Communications, Vol. 49, No. 4, April 2001

[11] T.M. Schmidl, D.C. Cox, "Low-Overhead, Low-Complexity Synchronization fir OFDM," IEEE International Conference on Communications, Vol. 3, 1996, pp 1301-1306

[12] Meng-Han Hsieh and Che-Ho Wei, "A Low-Complexity Frame Synchronization and Frequency Offset Compensation Scheme for OFDM Systems over Fading Channels," IEEE Transactions on Vehicular Technology, Vol. 48, No. 5, September 1999

[13] J. Terry and J. Heiskala, "OFDM Wireless LANs: A Theoretical and Practical Guide,"

[14] Alan V. Oppenheim, Ronald W. Schafer, and John R. Buck, "Discrete-time signal processing", 2nd edition, PRENTICE HALL SIGNAL PROCESSING SERIES, 1989, 1999

[15] J. G. Proakis, "Digital Communication," McGraw-Hill, Boston, 4th., 2001

[16] S. Haykin, "Communication Systems," John Wiley & Sons, New York, 4th, 2001

[17] Wan-Yi Lin, Wen-Rong Wu, "Channel Estimation and Multiuser Asychronization Interference Mitigation for IEEE 802.16e System," National Chiao-Tung University, July 2006